PARTICLE ACCELERATION IN PULSAR MAGNETOSPHERES

by

Kile B. Baker

National Aeronautics and Space Administration
Grant NGR 05-020-668

SUIPR Report No. 762

October 1978

INSTITUTE FOR PLASMA RESEARCH
STANFORD UNIVERSITY, STANFORD, CALIFORNIA

PARTICLE ACCELERATION IN PULSAR MAGNETOSPHERES

by

Kile B. Baker

National Aeronautics and Space Administration

Grant NGR 05-020-668

SUIPR Report No. 762

October 1978

Institute for Plasma Research
Stanford University
Stanford, California

PARTICLE ACCELERATION IN PULSAR MAGNETOSPHERES

Kile Barton Baker
September, 1978

Abstract

This study is concerned with the structure of pulsar magnetospheres and the acceleration mechanism for charged particles in the magnetosphere. We follow the pulsar model developed by P. A. Sturrock (1971) and assume that charged particles are accelerated from each polar cap of a pulsar. These particles produce gamma rays via curvature radiation which in turn produce electron-positron pairs which are ultimately responsible for the observed radio emission. This model requires large acceleration of the particles near the surface of the star.

The required acceleration has not been produced in earlier pulsar models. We have developed a theorem which shows that particle acceleration cannot be expected when the angle between the magnetic field lines and the rotation axis is constant (e.g. radial field lines). If this angle is not constant, however, acceleration must occur.

We have investigated the more realistic model of an axisymmetric neutron star with a strong dipole magnetic field aligned with the rotation axis. In this case acceleration occurs at large distances

from the surface of the star. The magnitude of the current can be determined from this model and is found to be the same as estimated by Sturrock (1971). In the case of non-axisymmetric systems the acceleration is expected to occur nearer the surface of the star.

ACKNOWLEDGEMENTS

I would like to thank Professor P.A. Sturrock for his constant interest in the pulsar problem and his careful guidance in the details of its solution. I also wish to thank Professors R.V. Wagoner and V. Petrosian for their comments and suggestions.

I want to specially thank Joshua Knight for his help with the innumerable computer problems that developed over the course of this investigation. In addition his well developed skepticism over simple solutions to complex problems has helped me avoid many attractive pitfalls.

Finally, I gratefully acknowledge the financial support from the National Aeronautics and Space Administration through grant NGL-05-020-668.

TABLE OF CONTENTS

SIGNATURES ii

ABSTRACT iii

ACKNOWLEDGEMENTS v

Chapter page

I. INTRODUCTION 1

discovery and early theories 1

II. THE MAGNETOSPHERE PROBLEM 7

the PCLC and PCFB models 7
Self-consistent Magnetospheres 14

III. MATHEMATICAL FORMULATION 18

Basic equations 18
The Basic Model and Acceleration Theorem 18
Dipole Co-ordinates 21
Boundary Conditions 23
Analytic and Numerical Solutions 26
The Non-linear Problem 26
One Dimensional Solution 31
Numerical Solution to the non-linear 1-D problem 35
Two Dimensional Solution 41

IV. DISCUSSION AND CONCLUSION 53

The Acceleration Problem 53
The charge separated model 53
The effects of pair production 55
The effects of particle inertia 56
Return currents: Is a pulsar charged? 57
The Radiation Problem 58
Conclusion 60

Appendix page

A. MATHEMATICAL DETAILS 62

Green Function for the second order perturbation 62

Exact Integration of the Non-linear Problem 63

B. COMPUTER LISTINGS 64

BIBLIOGRAPHY 69

LIST OF TABLES

Table page

1. Neutron Star vs. White Dwarf Models 3

2. Light Cylinder vs. Polar Cap Models 5

3. Equations and Boundary Conditions 26

4. Relative Phases of Radio, Optical, X-Ray, and Gamm Ray Pulses for four pulsars. 59

LIST OF FIGURES

Figure page

1. Basic picture of the magnetosphere of an axisymmetric rotating magnetic neutron star 8

2. Pulse Width vs. Period 13

3. γ vs $R/R_\star$ for η/η_{max}= 0,.48,.69,.83,.97 and j_{12}=1. Values of η/η_{max} are plotted from top to bottom 37

4. Accelerating electric field plotted vs. $r/R_\star$ for η/η_{max}=0,.48,.69,.83,.97 and j_{12}=1. 38

5. $\delta\equiv\gamma-1$ plotted vs. $\delta r/R_\star$ with η/η_{max}=0,.48,.69,.83,.97 and j_{12}=1. 39

6. γ plotted for various values of $j_\star$, with co-ordinate η=0. 40

Chapter I

INTRODUCTION

1.1 DISCOVERY AND EARLY THEORIES

> The discovery of the pulsars by Professor Hewish and Miss Jocelyn Bell in 1967 ranks with the discovery of quasars and of the universal microwave background radiation as one of the major advances in modern astronomy.
>
> F.G. Smith, Pulsars, p. xi

The discovery of pulsars aroused immediate and intense interest not only among astrophysicists and astronomers but the public as well. A number of attempts were quickly put forward to explain these remarkable objects. Perhaps the most popular with the general public was the so called "LGM" (Little Green Men) theory, which suggested that the pulses were signals from an advanced extra-terrestrial civilization. This theory, however, was quickly discounted; the signals were too regular; since the periods were unmodulated they carried no information and it was therefore highly unlikely that any little green men were using them as communications beacons. It was still possible that pulsars were some sort of galactic lighthouses but it was clear that astrophysicists would do well to look for a more natural (though less exciting) explanation.

The most immediately attractive idea was that pulsars were related to white dwarf stars and several theories were developed along these lines (e.g. Ginzburg et al. 1968; Black, 1969). At the same time, however, some work was being done on the possiblility that pulsars were related to neutron stars (Gold, 1968; Pacini, 1968). In fact, even before the first pulsar was discovered Pacini (1967) had suggested that a

magnetized rotating neutron star was responsible for the energy budget of the Crab Nebula. The controversy did not last long and was finally settled by the discovery of the Vela pulsar (Large, Vaughan and Mills, 1968) and the Crab pulsar (Staelin and Reifenstein, 1968), which had much shorter periods than previously discovered pulsars. The white dwarf theories were now running into serious difficulties, which are summarized in table 1 below. In the first place, it was clear that white dwarf stars could not be rotating with periods any faster than approximately 8 sec. (This is the period for which the gravitational force equals the centrifugal force at the surface of a white dwarf). Vibrational modes of a white dwarf could also be rejected. Since vibrational periods are approximately given by

$$P \simeq (G\rho)^{-1/2}, \qquad (1.1.1)$$

the expected pulsation period for white dwarfs is of the order of 1 sec, which fits reasonably well with the first discovered pulsars but is difficult to reconcile with the Crab or Vela periods. In addition, it is difficult to understand why only one mode is observed and why the mode is so stable. Furthermore, as a white dwarf ages it cools and contracts slightly. Thus the density increases and the vibrational period would be expected to decrease; instead pulsar periods are observed to increase, which is what one expects of a rotating system. Since white dwarf rotations must be rejected, we are left with neutron star rotations. Thus, with the discovery of the Vela and Crab pulsars, white dwarf models were no longer tenable and it was clear that neutron stars had finally been observed.

TABLE 1

Neutron Star vs. White Dwarf Models

	NS	WD
1. Period in range 0.03 to 3.7 s	√	X
2. Period stable to one part in 10^9	√	?
3. Period increases	√	X?
4. No optical photospheric radiation	√	X
5. Two pulsars in supernova remnants	√	X

Having determined that the pulses were due to the rotation of a neutron star it was now necessary to develop a more detailed model for the emission mechanism.

In a recent book of the subject of pulsars, Manchester and Taylor (1977) remark:

> One of the least understood aspects of pulsars is the mechanism by which rotational energy is converted into pulses we observe. Although numerous theoretical models for the emission mechanism have been proposed, no single model has been generally accepted.

It is clear that the emission mechanism must be a coherent one. The brightness temperature at a given frequency is defined by

$$T_b(\nu) = \frac{I(\nu)c^2}{2k\nu^2} \qquad (1.1.2)$$

For typical pulsar parameters this gives brightness temperatures in the

range of 10^{23} K to as high as $T_b = 10^{30}$ K. For incoherent processes this implies particle energies of the order of $kT_b \simeq 10^{26}$ eV. It is difficult to imagine an acceleration mechanism which will produce particles of such enormous energies and even if such such highly energetic particles were produced, they would radiate most of their energy in the frequency band around $5.8 \times 10^{10} T_b \simeq 5.8 \times 10^{40}$ Hz. Such energies have never been observed and we may therefore reject incoherent processes as the source of the radio emission. There have been many suggestions for the coherent mechanism, but none has been completely satisfying and I will have little more to say on this subject in this dissertation.

A second question must also be considered in relation to the radio emission. Where is the radiation produced? There are two main schools of thought on this question. The first (e.g. Gold, 1969) advocates the "light cylinder" model, in which plasma follows field lines out to the light cylinder. At the light cylinder, the plasma is highly relativistic and radiation is beamed in the forward direction. Light cylinder models were refined by F.G. Smith (1971 and 1973) but little recent theoretical work has been done to develop detailed pulsar models with emission at the light cylinder. The alternate model was initially presented by Radhakrishnan and Cooke (1969). In their model, the emission region is near the surface of the neutron star, in the region above the magnetic polar caps. The radiation is assumed to be beamed into a cone (known as the emission cone) and thus acts rather like a lighthouse beacon. The relative merits of these two pictures is still a subject of some controversy, but a partial summation is given in table 2 below.

TABLE 2

Light Cylinder vs. Polar Cap Models

Light Cylinder Models - Merits

1. Natural beaming process

2. Rapid, asymmetric changes in polarization within subpulses

Light Cylinder Models - Deficiencies

1. The strength of the magnetic field at the light cylinder depends on the pulsar period. Thus pulses from slow pulsars might be expected to be very different from pulses of fast pulsars. This is not observed.

2. The emission region is small compared to the light cylinder radius. A mechanism must be found continuously to supply particles to the emission region while maintaining the coherence of the process.

3. The stability of the pulse shapes indicates that the emission takes place in a region of strong magnetic fields where the particles co-rotate with the star. This is unlikely near the light cylinder.

Polar Cap Models - Merits

1. Simple explanation of the stability of even very complex pulse profiles.

2. The emission region would be expected to be small compared to the entire stellar surface thus producing pulses with widths of the order of 10° of longitude (as observed).

3. Strength of the magnetic field in the emission region is independent of the period and hence pulse characteristics would be expected to be relatively insensitive to period.

Polar Cap Models - Deficiencies

1. The simplest polar-cap models predict a pulse width that is smaller than observed.

2. Particles must be accelerated to highly relativistic

energies in order to produce and beam the radiation. But the charge density in the magnetosphere may be expected to adjust to decrease the acceleration (if possible).

3. The relation between energy loss and angular momentum loss suggests that the primary processes (energy and angular momentum loss) affecting the star must occur at the light cylinder (C.f. Holloway, 1977).

The one truly outstanding problem with polar-cap models is the source of the acceleration, which is required to produce coherent radio emission near the stellar surface. This dissertation is primarily devoted to an attempt to deal with that problem. In Chapter II, section 1 I will present the basic model in more detail, while section 2 will deal with an analysis of the problem of particle acceleration in polar-cap models. In Chapter III I present a new approach to the acceleration problem using a more realistic magnetic field structure than in previous work. Finally, in Chapter IV I discuss the results of this research.

Chapter II

THE MAGNETOSPHERE PROBLEM

2.1 THE PCLC AND PCFB MODELS

Before turning to the main body of this thesis it is necessary to define in more detail the salient features of the Stanford pulsar models, which form the basis of the current work. The original model was developed by P.A. Sturrock (1970,1971a,1971b) and has formed the basis of all subsequent development of pulsar models at Stanford. In 1969, P. Goldreich and W.H. Julian published a paper of fundamental importance to the pulsar problem. In this paper they demonstrated that "in spite of its intense surface gravity, the star must possess a dense magnetosphere." The plasma in the magnetosphere has essentially infinite conductivity and hence obeys the "frozen-in-flux" condition. The magnetic field lines may be viewed as being firmly attached to the surface of the neutron star and, as the star rotates, the plasma in the magnetosphere is forced to rotate along with it. This cannot, of course, be true if the plasma would be forced to move faster than the speed of light and hence at the light cylinder the "frozen-in-flux" condition requires that magnetic field lines be pulled out and wrapped around the star. The basic picture is shown in Figure 1 below.

The distance, R_Y, is the radius of the "Y-type neutral point" and it defines the field line which separates field lines that are closed within the co-rotating magnetosphere from lines that are (in some sense)

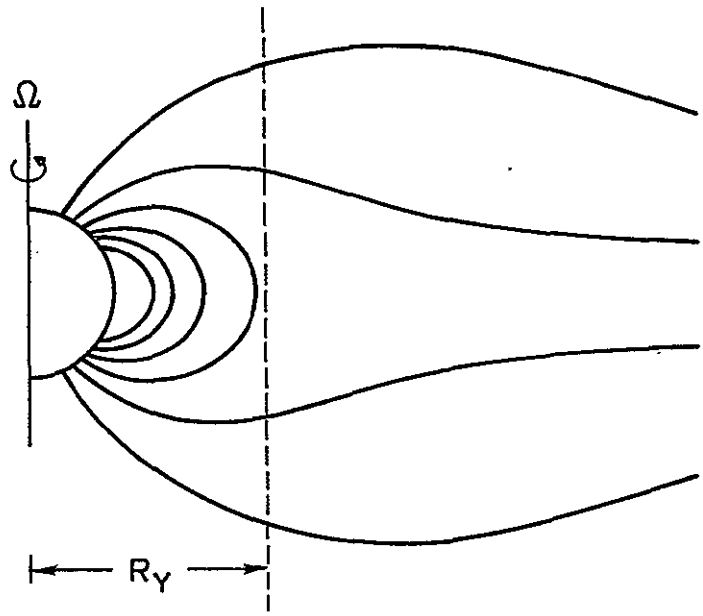

Figure 1: Basic picture of the magnetosphere of an axisymmetric rotating magnetic neutron star

open, and connect to the interstellar medium surrounding the star. In the Goldreich-Julian model (hereafter referred to as the G-J model) the radius R_L is the light cylinder radius defined by

$$R_y = R_L \equiv c/\Omega = cP/2\pi, \qquad (2.1.1)$$

where Ω is the angular frequency and P is the pulsar period. It is then assumed that particles flow freely along magnetic field lines (i.e.

$\underset{\sim}{E}\cdot\underset{\sim}{B} = 0$). This determines a charge density in the magnetosphere given by

$$\rho = -\frac{\underset{\sim}{\Omega}\cdot\underset{\sim}{B}}{2\pi c}\,\frac{1}{\left[1-\left(\frac{\Omega r}{c}\right)^2\sin^2\theta\right]} \qquad (2.1.2)$$

The model developed by Sturrock (referred to as the Polar Cap Light Cylinder model) (1970,1971a,1971b) is basically an extension of the work of Goldreich and Julian in which the condition that $\underset{\sim}{E}\cdot\underset{\sim}{B} = 0$ everywhere is relaxed. Specifically, the condition does not apply to the open field lines. Thus, on open field lines, particles can be accelerated to very large energies.

The polar cap is defined by the condition that the magnetic field line which leaves the edge of the cap be the last closed field line. Thus all field lines emanating from the polar-cap region are open field lines and particles may be accelerated along these field lines. The equation defining a dipole field line is

$$\sin^2\theta/r = \text{const.} \qquad (2.1.3)$$

The polar cap angle θ_p is then defined by

$$\sin^2\theta_p = R_*/R_L \qquad (2.1.4)$$

The rotation of the star induces a potential difference between the center of the polar cap and the edge. In the simple case of an aligned rotator, the potential on the surface of the star is then given by

$$\Phi_* = \frac{-\Omega B_* R_*^2}{2c}\cos^2\theta \qquad (2.1.5)$$

where B_* is the strength of the magnetic field at the pole and R_* is the

radius of the star. Then, from equations (2.1.4) and (2.1.5) we find that the potential difference from the center of the polar cap to the edge is

$$\Delta\Phi_* = -\frac{\Omega\, B_*\, R_*^2}{2c}\sin^2\theta_p = -\frac{\Omega\, B_*\, R_*^3}{2\, R_L\, c} \qquad (2.1.6)$$

For typical pulsar parameters this gives a potential difference of the order of 10^{16} Volts. Thus in this model we may expect charged particles to be rapidly accelerated to highly relativistic energies. In this model, each polar cap produces two current streams. In particular, if $\Omega\cdot B > 0$ electrons are accelerated from the central portion of the polar cap and ions are accelerated from an annulus around the central area. The two zones are referred to as the "electron polar zone" (EPZ) and the "ion polar zone" (IPZ) respectively.

Because the particles follow curved field lines, they emit photons of energies

$$\mathcal{E}(ev) \simeq 10^{-31.9}A^{-3}E^3R_c^{-1} \qquad (2.1.7)$$

where A is the mass in a.m.u. ($A=10^{-3.26}$ for electrons), E is the energy of the charged particle (in eV) and R_c is the radius of curvature of the field line. As the photons cross magnetic field lines, they "see" a changing, transverse magnetic field with which they can interact, producing electron-positron pairs (Erber, 1966; Daugherty and Lerche, 1976). In this model, the pair production process is necessary for the production of coherent radio emission. Clearly, for this mechanism to work, the initial gamma rays must have energies above the pair-production threshold, which in turn requires that the energy of the initial particles be above some threshold energy (dependent on the

curvature of the field lines). This then gives a natural explanation of the "turn-off" condition for pulsars. This condition has been further investigated by Sturrock,Baker and Turk (1976) and has been generalized to include radiation reaction and distorted magnetic fields.

This model (like most polar-cap models) predicted a definite relationship between the pulse width and pulsar period given by

$$W \propto P^{1/2} \tag{2.1.8}$$

As can be seen from figure 2, the PCLC model does not fit this distribution at all well. In addition, the PCLC model (along with most polar-cap models) predicts that the braking index defined by

$$n = \omega\ddot{\omega}/\dot{\omega}^2 \tag{2.1.9}$$

have the value n=3. It is very difficult to determine the braking index, but for the Crab pulsar the current best value is n=2.215±.005 (Groth, 1975).

This led D.H. Roberts and P.A. Sturrock (1972a,1972b,1973) to modify the PCLC model by changing the "Y-type neutral point" from the light cylinder radius, R_L, to the "force balance radius", R_{FB}, which is the radius at which the co-rotation velocity is the Keplerian velocity for a circular orbit (Roberts and Sturrock, 1972a, 1972b, 1973).

$$R_{FB} = (GM)^{1/3}\Omega^{-2/3} \tag{2.1.10}$$

In this model (called the PCFB model), the polar cap angle, θ_p ,is given by

$$\theta_p \simeq 10^{1.5}M^{-1/6}R_*^{1/2}P^{-1/3} \tag{2.1.11}$$

and hence the pulse width is proportional to $P^{2/3}$. As can be seen from figure 2, the fit is much better. In the region $r<R_{FB}$ the magnetic

field is assumed to vary as r^{-3} while in the region beyond R_{FB} the magnetic field varies as r^{-2}. This change in the magnetic field structure changes the torque and the braking index is then given by n=2.33, which is in better agreement with the observed value for the Crab pulsar.

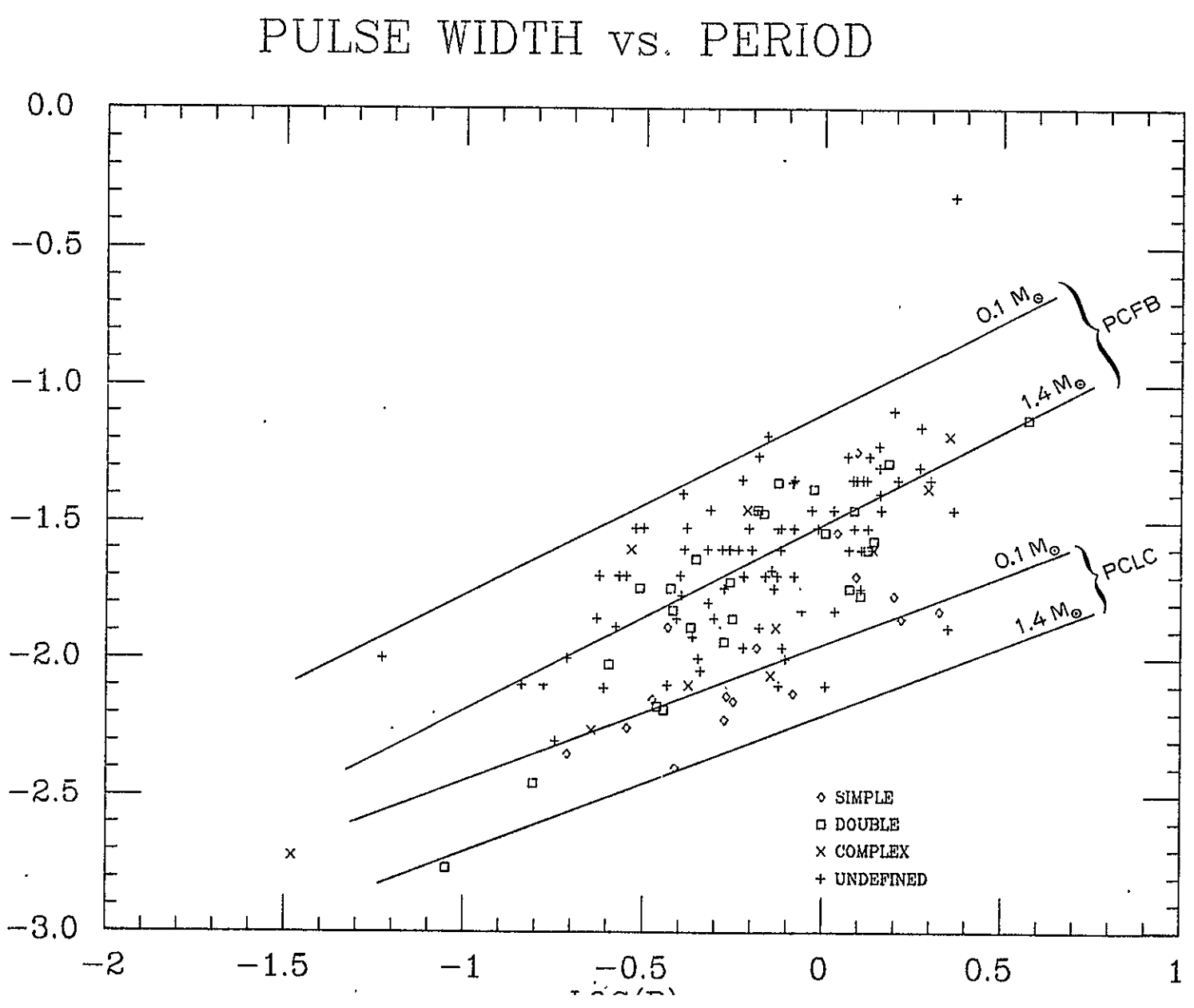

Figure 2: Pulse Width vs. Period

2.2 SELF-CONSISTENT MAGNETOSPHERES

The first comment that needs to be made on the subject of self-consistent magnetospheres is the limited use of the term "self-consistent." To be truly self-consistent, a model of pulsar magnetospheres would have to include a) the effects of currents in the magnetosphere on the magnetic field structure, b) the effects of particle masses on the currents which develop, and c) the effects (via the plasma) of radiation produced in the magnetosphere on its structure (e.g. radiation reaction, self absorption, scattering, etc.). That detailed a model is well beyond the scope of this thesis. By "self-consistent" we shall mean models which satisfy the appropriate equations without inducing large scale changes in the original conditions.

In 1974 N.J. Holloway published an important paper which illuminated some severe problems with the PCLC, PCFB, and similar pulsar models (e.g. Hinata, 1973; Hinata and Jackson, 1973). Holloway pointed out that there was a fundamental inconsistency in these models. Consider a cylindrical "gaussian pill-box" at the polar cap. The flux through the bottom surface is zero (space-charge limited flow), the flux through the top is nearly zero provided the "pill box" is extended far enough up to get it out of the accelerating region, and the flux through the sides is given by the co-rotation electric field $(\underset{\sim}{v}\times\underset{\sim}{B})$. The charge enclosed is therefore approximately

$$Q = -(\Omega\cdot B/2\pi c)\pi r_p^2 h \qquad (2.2.1)$$

where r_p is the radius of the polar cap and h is the height of the "pill-box". However, the currents from the EPZ and IPZ are expected to be comparable and the net charge enclosed should be approximately zero.

It is interesting to note, however, that the charge density is consistent with the current flow if only one sign of charge is accelerated. This suggests that instead of having currents of opposite charges both flowing out from the star, we may instead have a current loop, with the return current being outside of the polar-cap region.

It is possible that the large numbers of e^+-e^- pairs produced may adjust their distribution so as to satisfy equation (2.2.1) while the two currents flow through the pair plasma. The objection to such a model was well stated by Holloway:

> . . . in the positive particle acceleration zone of such a system, there would have to be an electric field which accelerated the positive particles to high energies, while leaving the negative particles essentially unmoved, a situation which, while perhaps not demonstrably impossible, (one could postulate a situation in which some form of plasma streaming instability counteracted the systematic fields) seems at least implausible. Furthermore, in the regions above the accelerating zones, the required coexistence of a relativistic, high density, stream of particles, with a static corotational charge density of the opposite sign, would seem to present great difficulties for this model.

M.A. Ruderman and P.G. Sutherland developed (1975) a new pulsar model which used a very clever idea. A fundamental point of the problem is the assumption that the accelerating electric field is zero on the stellar surface. Ruderman and Sutherland pointed out that if the work function of ions were high enough they could not be removed from the stellar surface. Thus, in the case that $\underset{\sim}{\Omega} \cdot \underset{\sim}{B} < 0$, so that ions must be removed from the central region of the polar cap, a vacuum region will develop (called the "polar gap") and a large accelerating electric field will form at the surface of the star (and in the entire "gap" region). In this model the accelerated particles come from the static breakdown of

the vacuum. Since this model relies on the work function for ions being very large, it requires that all pulsars have $\underset{\sim}{\Omega}\cdot\underset{\sim}{B} < 0$ (neutron stars with $\underset{\sim}{\Omega}\cdot\underset{\sim}{B} > 0$ would not accelerate particles and hence would not produce coherent radiation). The reason for the large work function for ions is that in a strong magnetic field ($\sim 10^{12}$ gauss) the ions form long chains and the gravitational binding of the chain is large. Recently, Flowers and his co-workers (including Sutherland) (Flowers, et al. 1977) have recalculated the work function and found that the work function used in the Ruderman-Sutherland pulsar model had been over-estimated by approximately an order of magnitude. With the new work-function estimate, the polar gap does not develop, and the net result is (in Sutherland's own words[1]) that "the model is dead."

Both F. Curtis Michel and E.A. Jackson have developed pulsar models which avoid Holloway's criticisms. They also, unfortunately, produce very little acceleration and provide no mechanism for the observed radiation. Michel's model (1975) utilizes currents of a single sign moving on radial field lines (see Chapter 3, section 1) and thus simply matches the G-J charge density. In the simplest form of the model (where particle inertia is ignored) no acceleration takes place at all. When the particle masses are taken into account there is acceleration until the particles become relativistic, at which point the acceleration ceases. Even in this case, the acceleration is not sufficient to provide a mechanism for the observed radiation. Typical values of the

---

[1]Private communication made to the author at the eighth Texas Symposium of Relativistic Astrophysics, Boston, MA., Dec. 1976.

relativity parameter γ are of the order of 10, compared to 10^{10} for the PCLC model.

Jackson's model (1976) abandons the requirement of space-charge limited flow and substitutes field emission (at T ~ 0 K) at the surface. The current is then related to the accelerating electric field by

$$j_* = [6.2\times10^{-6}E_{\parallel}^2(\mu/\phi)^{1/2}/(\phi+\mu)]\exp[-6.8\times10^{7}\phi^{3/2}/E_{\parallel}] \qquad (2.2.2)$$

where $E_{\parallel}$ is in volts/cm, ϕ is the work function in eV, and μ is the Fermi energy relative to the bottom of the conduction band. This model also features complete current loops, so the requirement of zero net current leaving the star can be dropped (since no current at all leaves the star). The difficulty is, again, that there is very little acceleration and no reasonable radiation mechanism.

Chapter III

MATHEMATICAL FORMULATION

3.1 BASIC EQUATIONS

3.1.1 The Basic Model and Acceleration Theorem

The pulsar model presented here is a development of the polar-cap models of Sturrock and Roberts and Sturrock (see Chapter II, section 1). Fundamental to this model is the fact that currents flow from the polar cap along magnetic field lines. That this is true can be demonstrated by comparing the gyroradius of the particles with the radius of the polar cap. The gyroradius is given by

$$r_g = pc/eB \simeq \mathcal{E}/eB \simeq \Delta\Phi/B \qquad (3.1.1)$$

If we take the maximum $\Delta\Phi$ that we can get (equation 2.1.6) we find

$$r_g = \frac{\Omega^2 R_*^3}{2c} \frac{B_*}{B} \qquad (3.1.2)$$

Near the polar cap $B \simeq B_*$ and the polar cap radius is given by

$$r_p = \frac{R_*^{3/2}}{R_L^{1/2}} = \frac{R_*^{3/2} \Omega^{1/2}}{c^{1/2}} \qquad (3.1.3)$$

and hence the ratio of r_g/r_p is

$$\frac{r_g}{r_p} = \frac{1}{2} \left(\frac{\Omega R_*}{c}\right)^{3/2} = \frac{1}{2}\left(\frac{v_s}{c}\right)^{3/2} \sim 10^{-6} \qquad (3.1.4)$$

where v_s is the rotational velocity of the stellar surface. We note, however, that as $r \to R_L$, $r_g \sim R_L$. We can also estimate whether the magnetic field controls the current flow or whether the current flow

controls the structure of the magnetic field. For this we simply compare the energy density due to the kinetic energy of the particles to the energy density of the magnetic field. The particle number density is given by

$$n = \rho/e \cong \Omega B/(2\pi ce) \tag{3.1.5}$$

For the energy we again use $e\Delta\Phi$. Thus the ratio of kinetic to magnetic energies is estimated to be

$$\frac{KE}{B^2/8\pi} = \frac{2\Omega^3 R_*^3}{c^3} \quad \frac{B_* B}{B^2} = 2\left(\frac{\Omega R_*}{c}\right)^3 \times \left(\frac{r}{R_*}\right)^3 \tag{3.1.6}$$

Near the polar cap the ratio is very small ($\sim 10^{-12}$) and the magnetic field controls the particle flow. When r grows to the order of R_L however, the ratio approaches unity and in that region we may expect the magnetic field to be distorted by the particle flow.

We assume that the plasma is completely charge separated, which means that the pair production process is not taken into account in investigating the acceleration mechanism. This treatment would also be valid provided the net current due to pairs is small compared to the primary current from the polar cap. If the acceleration is large this will clearly not be the case and in the region of large pair production the model will break down (see Chapter IV). Since the particles are tied to magnetic field lines, the current density is proportional to the magnetic field strength. Thus, along a field line we may write

$$j(s) = j(0)[B(s)/B(0)] \tag{3.1.7}$$

where s is a co-ordinate along the field line and s=0 refers to the surface of the neutron star. Since the particles are relativistic (as

will be demonstrated in section 2), the charge density is given by

$$\rho \simeq \frac{j_* B}{c B_*} \qquad (3.1.8)$$

The G-J charge density (equation 2.1.2), which is required for $\underset{\sim}{E}\cdot\underset{\sim}{B}=0$ (i.e. no acceleration), is proportional to $\underset{\sim}{\Omega}\cdot\underset{\sim}{B}$. Thus, if the angle between $\underset{\sim}{\Omega}$ and $\underset{\sim}{B}$ is constant along a field line then equation (3.1.8) is compatible with (2.1.2) (in the non-relativistic limit) and it is therefore possible to have steady current flow with no acceleration. If, however, field lines curve then acceleration (or deceleration) must take place. This theorem has been independently derived by Arons, Fawley and Scharlemann (1978) by transforming to a rotating reference frame[2]. In the frame rotating with the star, there is an electric field perpendicular to the magnetic field, given by (in the non-relativistic limit)

$$\underset{\sim}{E}_{rot} \simeq [(\underset{\sim}{\Omega} \times \underset{\sim}{r}) \times \underset{\sim}{B}]/c \qquad (3.1.9)$$

If we assume that $\underset{\sim}{B}$ is approximately curl free (i.e. the magnetic field of the star is much larger than the field generated by currents in the magnetosphere), then the charge density of $\underset{\sim}{E}_{rot}$ is given by the G-J charge density (equation 2.1.2). We may then divide the electric field into two parts, the rotational part given by equation (3.1.9) and the non-rotational part which may accelerate particles. Thus only the difference between the rotational charge density and the true charge

---

[2]Tademaru (1974) proved a restricted version of the theorem, too. He showed that for an axisymmetric rotating system with a polar-cap region bounded by radial (i.e. monopole like) field lines, the component of E parallel to the magnetic field lines must be exactly zero.

density is a source of acceleration (Michel, 1975). When the angle between $\underset{\sim}{\Omega}$ and $\underset{\sim}{B}$ is constant we can find a current flow such that the non-rotational charge density is zero everywhere. When the angle is not constant, however, that is no longer possible and hence a non-rotational electric field must develop. We are thus motivated to look at a pulsar model in which the field lines are curved. The simplest physically realistic example is a pure dipole field.

3.1.2 Dipole Co-ordinates

In order to study the dipole field case we first introduce a co-ordinate system based on the dipole field lines. The potential of a magnetic dipole oriented along the z axis is given by $\Phi \propto \cos\theta / r^2$. The equation of a field line is $\sin^2\theta/r = \text{const}$. Thus for our co-ordinates we may take

$$\xi = \sqrt{\cos\theta/r} \quad \text{and} \quad \eta = \sin\theta/\sqrt{r} \tag{3.1.10}$$

The third co-ordinate is the azimuthal angle ϕ but we shall usually assume azimuthal symmetry and thus reduce the problem to two dimensions. The Laplacian for dipole co-ordinates can be written as

$$\nabla^2\Phi = \frac{\left(1 - \frac{3}{4} r \eta^2\right)}{r^6 \xi} \left[\frac{\partial}{\partial\xi}\left(\frac{1}{\xi}\frac{\partial\Phi}{\partial\xi}\right) + \frac{\xi}{\eta}\frac{\partial}{\partial\eta}\left(r^3\eta\frac{\partial\Phi}{\partial\eta}\right)\right] \tag{3.1.11}$$

Unfortunately, the values of r and θ cannot be expressed explicitly in terms of ξ and η, so the Laplacian cannot be written simply in terms of the dipole co-ordinates.

The polar-cap region is defined as the region of open field lines. The bounding field line is determined by the value of R_y, the "Y-type

neutral point" (see equation 2.1.11). Thus we can define a maximum value for the co-ordinate η by

$$\eta_{max} = R_y^{-1/2} \tag{3.1.12}$$

Since we are assuming a charge separated plasma, the current density is given by

$$\underset{\sim}{j}(r) = \rho(r)\underset{\sim}{v}(r) \tag{3.1.13}$$

Since the particles are tied to field lines, $\underset{\sim}{j}$ can be separated into two components, the motion along the field line and the motion due to the rotation of the star. However, motion due to rotation is small compared to that along field lines if $r \ll R_L$ (the light cylinder). We shall therefore neglect the rotation part of the current density, in which case equation (3.1.13) becomes a scalar equation. Combining it with equation (3.1.7) we then have

$$\rho(\xi,\eta) \simeq \frac{j_*(\eta)}{v(\xi,\eta)} \quad \frac{|\underset{\sim}{B}(\xi,\eta)|}{|\underset{\sim}{B}(\xi_*,\eta)|} \tag{3.1.14}$$

where ξ_* is the value of ξ on the surface of the star ($\xi_* \simeq 1/R_*$) and v is the velocity of the particles. Since the field is dipolar, we can write $B(\xi,\eta)$ as

$$B(\xi,\eta) = \frac{2\mu}{r^3}\left(1 - \frac{3}{4} r \eta^2\right)^{1/2} \tag{3.1.15}$$

where μ is the dipole moment and r is implicitly determined by ξ and η. Combining equations (3.1.14) and (3.1.15) we then have

$$\rho(\xi,\eta) = \frac{j_*(\eta)}{v(\xi,\eta)} \left(\frac{R_*}{r}\right) \left[\frac{1 - \frac{3}{4} r\eta^2}{1 - \frac{3}{4} R_* \eta^2}\right]^{1/2} \tag{3.1.16}$$

For many purposes we can ignore the $r\eta^2$ dependence entirely. Since $r\eta^2 \leq 1$ we can make the expansion

$$\left(1 - \frac{3}{4} r\,\eta^2\right)^{1/2} \simeq 1 - \frac{3}{8} r\,\eta^2 \qquad (3.1.17)$$

and even at the extreme value of $r\eta^2 = 1$ ($\theta = \pi/2$) we make an error of no more than 25%.

3.1.3 Boundary Conditions

We must now consider the boundary conditions appropriate to the problem. One boundary condition is clear: the bounding closed field line satisfies the condition $\underset{\sim}{E}\cdot\underset{\sim}{B} = 0$ and hence the potential along the field line must be a constant, which we may take to be zero. In terms of dipole co-ordinates we therefore have

$$\Phi(\eta_{max}) = 0. \qquad (3.1.18)$$

(Unless otherwise stated, Φ refers to the electric potential.) The surface of a neutron star is a good conductor and therefore the Lorentz force on a charged particle on the rotating surface must be zero. Hence the electric field parallel to the stellar surface must be the rotation electric field (equation 3.1.9). If we assume that $\underset{\sim}{B}$ is the gradient of a potential with azimuthal symmetry, we can write

$$\Phi_M = \sum_{\ell=1}^{\infty} \mu_\ell \frac{P_\ell(\cos\Theta)}{r^{\ell+1}} \qquad (3.1.19)$$

for the magnetic potential, where μ is the moment associated with the ℓ-pole. Thus Φ, the electric potential can be determined on the conductor surface by

$$\Phi = -R_* \int [(\Omega \times r) \times \nabla \Phi_M] d\theta \qquad (3.1.20)$$

If the rotation axis is aligned with the symmetry axis of the magnetic field this is easy to integrate. Since the velocity of the surface is entirely in the ϕ direction we need only consider the radial derivative of the magnetic potential. We then find that the electric potential is given by

$$\Phi_E = -\sum_{\ell=1}^{\infty} \left(\frac{4\pi}{2\ell+1}\right)^{1/2} \frac{\Omega\mu_\ell}{c} \frac{\ell+1}{2\ell+1} \frac{P_{\ell+1}(\cos\theta) - P_{\ell-1}(\cos\theta)}{R_*^\ell} \qquad (3.1.21)$$

In the case of a pure dipole magnetic field this becomes

$$\Phi = -\Omega B_* R^2(\cos^2\theta - \cos^2\theta_p)/2c. \qquad (3.1.22)$$

In terms of the dipole co-ordinates we may rewrite this as

$$\Phi_E = -\frac{\Omega\, B_*\, R_*^3\, \eta_{Max}^2}{2c}\left(1 - \frac{\eta^2}{\eta_{Max}^2}\right) \qquad (3.1.23)$$

The remaining boundary condition is more difficult to determine. Typically, the remaining boundary condition would be at infinity ($r=\infty$). In the case of dipole field lines, however, the field lines do not extend to infinity. Nevertheless, at $r=\infty$ it is true that $\xi=0$ but ξ is also zero at $\theta=\pi/2$. The dipole field structure must breakdown at the light cylinder (or perhaps at some $R_y < R_L$) and the "frozen-in-flux" condition also breaks down when $E \geq B$, a condition we may again expect near the "Y-type neutral point." This indicates that we should be looking for a boundary condition which applies at the point $r=R_y$. If the "frozen-in-flux" condition breaks down at R_y it is no longer reasonable to assume $\underset{\sim}{E}_\perp \simeq -\underset{\sim}{v}/c \times \underset{\sim}{B}$. In addition, since $B \sim r^{-3}$ up to the radius R_y, $B(R_y) << B_*$. Therefore (as pointed out at the beginning of

this chapter), the gyroradius is comparable to R_y and particles can cross field lines, effectively shorting out the circuit. Hence we may consider the approximation that $\underset{\sim}{E}_\perp \sim 0$ at R_y and therefore the electric potential is approximately constant at R_y. Since this surface intersects with the bounding field lines, on which the potential is zero we must have

$$\Phi(R_y,\theta) \simeq 0 \qquad (3.1.24)$$

which then provides a complete set of Dirichlet boundary conditions.

There is one additional condition, however, that we may be able to apply. At the surface of the star (where particle flow is not relativistic) a region of charge may develop which then decreases the electric field normal to the surface. This phenomenon is well known from vacuum tube technology and is known as "space-charge limited flow". If the accelerating field were non-zero at the surface we would expect the current flow to be increased (a stronger electric field would pull out more particles) and hence the charge density would increase. Steady flow is achieved when the current flow is just sufficient to keep the accelerating field zero at the point of particle emission. Space-charge limited flow is an important feature of the PCLC and PCFB models and has also been invoked by many other investigators (though not all, e.g. Jackson,1976). Thus as an additional constraint on the problem we will consider the case of space-charge limited flow, which implies that the accelerating electric field at the surface must be zero.

$$\partial\Phi/\partial\xi \,\big|_{\xi_*} = 0 \qquad (3.1.25)$$

We how have an overdetermined problem and we are no longer free to choose the initial current density at the surface of the star. The equations and boundary conditions are collected in table 3.

TABLE 3

Equations and Boundary Conditions

$$\rho(\xi,\eta) = \frac{j_*(\eta)}{\dot{v}(\xi,\eta)} \left(\frac{R_*}{r}\right)^3 \left[\frac{1 - \frac{3}{4} r\eta^2}{1 - \frac{3}{4} R_*\eta^2}\right]^{1/2} \qquad (3.1.16)$$

$$\frac{1 - \frac{3}{4} r\eta^2}{r^6 \xi} \left[\frac{\partial}{\partial \xi}\left(\frac{1}{\xi}\frac{\partial \tilde{\Phi}}{\partial \xi}\right) + \frac{\xi}{\eta}\frac{\partial}{\partial \eta}\left(r^3 \eta \frac{\partial \tilde{\Phi}}{\partial \eta}\right)\right] = -4\pi\rho(\xi,\eta) \qquad (3.1.11)$$

$$\tilde{\Phi}(\xi,\eta_{Max}) = 0 \qquad (3.1.18)$$

$$\tilde{\Phi}(R_Y,0) = 0 \qquad (3.1.24)$$

$$\tilde{\Phi}(\xi_*,\eta) = -\frac{\Omega B_* R_*^3 \eta_{Max}^2}{2c}\left(1 - \eta^2/\eta_{Max}^2\right) \qquad (3.1.23)$$

$$\left.\frac{\partial \tilde{\Phi}(\xi,\eta)}{\partial \xi}\right|_{\xi_*} = 0 \qquad (3.1.25)$$

3.2 ANALYTIC AND NUMERICAL SOLUTIONS

3.2.1 The Non-linear Problem

We will first show that the particles from the polar cap are quickly accelerated to relativistic velocities. In this analysis we will consider a one-dimensional model (that is, assume the divergence of E across field lines can be neglected with respect to the divergence along

the field lines) and a small angle approximation. Poisson's equation is non-linear in this case because the velocity in equation (3.1.16) is dependent on the potential. Rather than work with the potential we shall work directly with the particle energy.

$$\mathcal{E} = \gamma m_0 c^2 = m_0 c^2 - e\Phi + \text{const.} \tag{3.2.1}$$

so

$$\nabla^2 \Phi = -(m_0 c^2/e)\nabla^2 \gamma \tag{3.2.2}$$

The velocity can be expressed in terms of γ as

$$v = \frac{(\gamma^2 - 1)^{1/2}}{\gamma} \, c \tag{3.2.3}$$

and hence Poisson's equation reduces to

$$\nabla^2 \gamma \simeq \frac{4\pi e}{m_0 c^2} \, \frac{j_*}{R} \left(\frac{R_*}{r}\right)^3 \left[\frac{1 - \frac{3}{4} r \eta^2}{1 - \frac{3}{4} R_* \eta^2}\right]^{1/2} \frac{\gamma}{(\gamma^2 - 1)^{1/2}} \tag{3.2.4}$$

We now assume that (at least until the motion becomes relativistic) the divergence of the electric field along the magnetic field lines is much greater than the divergence of the electric field perpendicular to the magnetic field lines. Thus η derivatives can be ignored. We also make a small angle approximation and ignore $r\eta^2$ terms. Equation (3.2.4) then becomes

$$\frac{1}{r^3} \frac{d}{dr} \left(r^3 \frac{d\gamma}{dr}\right) \simeq \frac{4\pi e}{m_0 c^2} \, \frac{j_*}{c} \left(\frac{R_*}{r}\right)^3 \frac{\gamma}{(\gamma^2 - 1)^{1/2}} \tag{3.2.5}$$

where the dipole nature of the field lines is reflected by the r^3 dependence. Equation (3.2.5) cannot be solved analytically and so additional approximations must be made. The necessary approximation is

to assume a cylindrical model for the structure of the magnetic field lines near the surface. Thus equation (3.2.4) becomes

$$\frac{d^2\gamma}{dr^2} \simeq \frac{4\pi e}{m_0 c^2} \frac{j_*}{c} \left(\frac{R_*}{r}\right)^3 \frac{\gamma}{(\gamma^2-1)^{1/2}} \tag{3.2.6}$$

This can be integrated once by multiplying both sides of Poisson's equation by $d\gamma/dr$ giving us

$$\frac{d\gamma}{dr} = \left[\frac{8\pi e j_*}{m_0 c^3}\right]^{1/2} \left(\frac{R_*}{r}\right)^{3/2} (\gamma^2-1)^{1/4} \tag{3.2.7}$$

This may then be integrated in terms of elliptic integrals. We first make the substitution

$$\cosh y = \gamma \,. \tag{3.2.8}$$

Then the solution to equation (3.2.7) is given (implicitly) by

$$\begin{aligned} &\frac{2(\sinh y)^{1/2} \cosh y}{1 + \sinh y} + F\left(\alpha, \frac{1}{\sqrt{2}}\right) - 2E\left(\alpha, \frac{1}{\sqrt{2}}\right) \\ &= 2\left[\frac{8\pi e j_*}{m_0 c^3}\right]^{1/2} R_*^{3/2} \left[\frac{1}{\sqrt{R_*}} - \frac{1}{\sqrt{r}}\right] \end{aligned} \tag{3.2.9}$$

where F and E are elliptic integrals of the first and second kind respectively, and

$$\alpha = \arccos\left(\frac{1 - \sinh y}{1 + \sinh y}\right) = \arccos\left(\frac{1 - \sqrt{\gamma^2-1}}{1 + \sqrt{\gamma^2-1}}\right) \tag{3.2.10}$$

We must remember, however, that this equation is valid only for $r \simeq R_*$

so that the divergence of the field lines could be ignored. Rather than working with the full analytic result, it is easier to consider the additional approximation that $\gamma \simeq 1$ (i.e. non-relativistic motion). We therefore write

$$\gamma = 1 + \delta \tag{3.2.11}$$

and keep only terms to first order in δ. Equation (3.2.7) then becomes

$$\frac{d\delta}{dr} \simeq \left[\frac{8\pi e j_*}{m_0 c^3}\right]^{1/2} \left(\frac{R_*}{r}\right)^{3/2} 2^{1/4}\, \delta^{1/4} \tag{3.2.12}$$

Integrating, we find

$$\frac{4}{3}\,\delta^{3/4} \simeq 2^{5/4} \left[\frac{8\pi e j_*}{m_0 c^3}\right]^{1/2} R_*^{3/2} \left[\frac{1}{\sqrt{R_*}} - \frac{1}{\sqrt{r}}\right] \tag{3.2.13}$$

and since we know $r \simeq R_*$ we can further approximate the right hand side to get

$$\frac{4}{3}\,\delta^{3/4} \simeq 2^{1/4} \left[\frac{8\pi e j_*}{m_0 c^3}\right]^{1/2} (\delta r) \tag{3.2.14}$$

where $r = R_* + \delta r$ and $\delta r \ll R_*$. Finally, we can solve for δ to get

$$\delta \simeq \frac{3^{4/3}}{2^{1/3}} \left[\frac{\pi e j_*}{m_0 c^3}\right]^{2/3} (\delta r)^{4/3} \tag{3.2.15}$$

Typical estimates for the current are of the order of 10^{12} esu/cm^2-sec. Thus, we write equation (3.2.15) in the form

$$\delta \simeq .56\, j_{12}^{2/3} (\delta r)^{4/3} \tag{3.2.16}$$

where we have assumed the particles are electrons and where

$j_{12} = j_* \times 10^{-12}$ and δr is measured in centimeters. In the non-relativistic limit, $\delta \simeq \frac{1}{2}\beta^2$ and hence when $\delta \simeq \frac{1}{2}$ the particles have velocity $v \simeq c$ and the non-relativistic approximation is no longer valid. It is clear from equation (3.2.16) that the particle becomes relativistic within a few centimeters to a few meters (depending on the magitude of j_*). We can also estimate the distance over which the divergence of the field lines becomes significant. From the approximate solution (equation 3.2.15) we find that

$$\frac{d\hat{\theta}}{dr} \simeq \frac{4}{3}\hat{\theta}\,(\delta r)^{-2/3} \qquad (3.2.17)$$

For typical pulsar parameters, Poisson's equation now can be written approximately as

$$\frac{d^2\hat{\theta}}{dr^2} \simeq 0.3\,(\delta r)^{-2/3} - 2 \times 10^{-6}\,(\delta r)^{2/3} \qquad (3.2.18)$$

where the second term on the right hand side had previously been ignored. The second term becomes comparable to the first when $\delta r \simeq 7 \times 10^4$ cm. Thus it is valid to ignore the divergence of the field lines in the non-relativistic limit.

Having confirmed that the particles quickly become relativistic, it is now possible to deal with a linear partial differential equation by simply replacing v with c in Poisson's equation, which now becomes (in

dipole co-ordinates)

$$\frac{(1 - \frac{3}{4} r\eta^2)}{r^6 \xi} \left[\frac{\partial}{\partial \xi} \left(\frac{1}{\xi} \frac{\partial \Phi}{\partial \xi} \right) + \frac{\xi}{\eta} \frac{\partial}{\partial \eta} \left(r^3 \eta \frac{\partial \Phi}{\partial \eta} \right) \right] \qquad (3.2.19)$$

$$= - \frac{4\pi j_*(\eta)}{c} \left(\frac{R_*}{r} \right)^3 \left[\frac{1 - \frac{3}{4} r\eta^2}{1 - \frac{3}{4} R_* \eta^2} \right]^{1/2}$$

3.2.2 One Dimensional Solution

As a first approach to the linear Poisson equation we again consider a one-dimensional approximation; that is we wish to consider the case where the divergence of $\underset{\sim}{E}$ perpendicular to the field lines is small compared to the divergence of $\underset{\sim}{E}$ along field lines.

$$|\nabla \cdot \underset{\sim}{E}_\perp| \ll |\nabla \cdot \underset{\sim}{E}_\parallel| \qquad (3.2.20)$$

We recall (equation 2.1.2) that the charge density for the case of $\underset{\sim}{E}_\parallel = 0$ (no acceleration) is proportional to $\underset{\sim}{\Omega} \cdot \underset{\sim}{B}$. This suggests that we look at the perpendicular rotator, for which case $\underset{\sim}{\Omega} \cdot \underset{\sim}{B} \simeq 0$. In this case, a significant departure from $j_\star = 0$ must indicate an accelerating electric field. We note that the one-dimensional model must be treated as an initial value problem rather than a boundary value problem. Before proceeding we also note that because the co-rotation charge density is approximately zero near the polar cap, any charge density due to the emitted current supports the accelerating field rather than the co-rotation field. This would tend to indicate that the acceleration probably occurs closer to the star surface in this case than is the

general rule. Equation (3.2.19) now reduces to

$$\frac{\left(1 - \frac{3}{4} r \eta^2\right)}{r^6 \xi} \frac{\partial}{\partial \xi}\left(\frac{1}{\xi} \frac{\partial \Phi}{\partial \xi}\right) \simeq - \frac{4\pi j_*}{c}\left(\frac{R_*}{r}\right)^3 \left[\frac{1 - \frac{3}{4} r \eta^2}{1 - \frac{3}{4} R_* \eta^2}\right]^{1/2} \tag{3.2.21}$$

Simplifying this equation we then find

$$\frac{\partial}{\partial \xi}\left(\frac{1}{\xi} \frac{\partial \Phi}{\partial \xi}\right) \simeq - \frac{4\pi j_*}{c} \frac{R_*^3}{\left(1 - \frac{3}{4} R_* \eta^2\right)^{1/2}} r^2 (\cos \theta)^{1/2} \left(1 - \frac{3}{4} r \eta^2\right)^{-1/2} \tag{3.2.22}$$

This can be integrated once exactly by integrating along a field line. Since $\partial\Phi/\partial\xi = 0$ on the surface, we have

$$\frac{1}{\xi} \frac{\partial \Phi}{\partial \xi} \simeq - \frac{4\pi j_* R_*^3}{c\left(1 - \frac{3}{4} R_* \eta^2\right)^{1/2}} \int_{\xi_*}^{\xi} r^2 (\cos \theta)^{1/2} \left(1 - \frac{3}{4} r \eta^2\right)^{1/2} d\xi \tag{3.2.23}$$

From the definitions of ξ and η, we may write the differentials

$$d\xi = - \frac{\sqrt{\cos \theta}}{r^2} dr - \frac{\sin \theta}{2r\sqrt{\cos \theta}} d\theta$$

$$d\eta = - \frac{\sin \theta}{2r^{3/2}} dr + \frac{\cos \theta}{r^{1/2}} d\theta \tag{3.2.24}$$

We know $d\eta = 0$ along a field line, and we can therefore express $d\theta$ in terms of dr to give us

$$d\xi = - \frac{\left(1 - \frac{3}{4} r \eta^2\right)}{r^2 (\cos \theta)^{3/2}} dr \tag{3.2.25}$$

Thus equation (3.2.23) becomes

$$\frac{1}{\xi}\frac{\partial\Phi}{\partial\xi} \simeq -K\int_{R_*}^{r} \frac{(1-\frac{3}{4}r\eta^2)^{1/2}}{\cos\theta}\,dr \qquad (3.2.26)$$

where

$$K = -\frac{4\pi j_* R_*^3}{c(1-\frac{3}{4}R_*\eta^2)^{1/2}} \qquad (3.2.27)$$

Along the field line $\cos\theta = (1-r\eta^2)^{1/2}$ so we then have

$$\frac{1}{\xi}\frac{\partial\Phi}{\partial\xi} \simeq -K\int_{R_*}^{r} \frac{(1-\frac{3}{4}r\eta^2)^{1/2}}{(1-r\eta^2)}\,dr \qquad (3.2.28)$$

and hence

$$\frac{1}{\xi}\frac{\partial\Phi}{\partial\xi} \simeq -K\left\{-(1-\tfrac{3}{4}r\eta^2)^{1/2}(1-r\eta^2)^{1/2} + \frac{1}{8}\log\frac{\left[(1-\frac{3}{4}r\eta^2)^{1/2}(1-r\eta^2)^{1/2} - (1-\frac{3}{4}r\eta^2)\right]^2}{1-\frac{3}{4}r\eta^2}\right\}\Bigg|_{R_*}^{r} \qquad (3.2.29)$$

This is not, however, a particularly useful form. Since we cannot expect the one-dimensional approximation to be valid for large r (and hence large θ) it is more useful to return to equation (3.2.28) and

expand to second order in θ (i.e. $r\eta^2$). We then have

$$\frac{1}{\xi}\frac{\partial\Phi}{\partial\xi} \simeq K\int_{R_*}^{r}\left(1 + \frac{1}{8}\, r\, \eta^2\right) dr \simeq K\left[(r - R_*) + \frac{\eta^2}{16}\,(r^2 - R_*^2)\right] \qquad (3.2.30)$$

It is now easy to do the next integration to order θ^2. We note that

$$d\xi = -dr/r^2 + \quad (\theta^4) \qquad (3.2.31)$$

and

$$\xi \simeq \frac{1}{r}\left(1 - \frac{1}{4}\, r\, \eta^2\right) \qquad (3.2.32)$$

Thus

$$\Delta\Phi \simeq -K\left\{\frac{1}{2R_*} - \frac{1}{r}\left(1 - \frac{1}{2}\,\frac{R_*}{r}\right) + \frac{\eta^2}{4}\left[-\frac{3}{4}\log\frac{r}{R_*} + \left(1 - \frac{R_*}{r}\right) - \frac{1}{8}\left(1 - \frac{R_*^2}{r^2}\right)\right]\right\} \qquad (3.2.33)$$

To zero order in η^2 we then have

$$\underset{\sim}{E}_{\parallel} \simeq +\frac{d\Phi}{dr}\,\hat{\xi} \simeq K\left[\frac{1}{r^2} - \frac{R_*}{r^3}\right]\hat{\xi} \qquad (3.2.34)$$

It is interesting to note that the electric field has a maximum at $r \simeq 1.5R_*$, which suggests that the maximum particle acceleration may occur at distances of the order of a stellar radius above the polar cap rather than at distances of the order of the polar cap radius as in most previous models. We further note that this form for $\underset{\sim}{E}_{\parallel}$ is due to the dipole nature of the field lines and is not found in cases where the field lines are not curved.

3.2.3 Numerical Solution to the non-linear 1-D problem

We now turn to a numerical solution to the non-linear one-dimensional model. The equation we wish to solve numerically is

$$\frac{\left(1 - \frac{3}{4} r \eta^2\right)}{r^6 \xi} \left[\frac{\partial}{\partial \xi}\left(\frac{1}{\xi}\frac{\partial \gamma}{\partial \xi}\right)\right]$$

$$= \frac{4\pi e j_*}{m_0 c^3}\left(\frac{R_*}{r}\right)^3 \left[\frac{1 - \frac{3}{4} r \eta^2}{1 - \frac{3}{4} R_* \eta^2}\right]^{1/2} \frac{\gamma}{(\gamma^2 - 1)^{1/2}} \qquad (3.2.35)$$

This equation can be solved easily using standard differential equation solving programs (in this case the program ODE, developed by Shampine and Gordon - see Appendix B - was used) provided accurate starting values can be determined. The infinity at $\gamma=1$ must be avoided by starting the integration at a position slightly above the stellar surface, where $\gamma=1+\delta$. The results of the first section are used to determine the starting values. The second order equation must first be decomposed into a pair of first order coupled equations.

$$\gamma_1 \equiv \gamma$$

$$\frac{d\gamma_1}{d\xi} = \gamma_2 \qquad (3.2.36)$$

$$\frac{d\gamma_2}{d\xi} = \frac{4\pi e j_*}{m_0 c^3} \frac{R_*^3 r^3 \xi^2}{\left(1 - \frac{3}{4} R_* \eta^2\right)^{1/2}} \frac{1}{\left(1 - \frac{3}{4} r \eta^2\right)^{1/2}} \frac{\gamma_1}{(\gamma_1^2 - 1)^{1/2}} + \frac{\gamma_2}{\xi}$$

We now rewrite the system in numerical terms.

$$\frac{d\gamma_1}{d\xi} = \gamma_2$$

$$\frac{d\gamma_2}{d\xi} = \frac{2.45 \times 10^{17}\, j_{12}\, R_{*6}^3\, r^3\, \xi^2\, \gamma_1}{\left[1 - .75 \times 10^6\, R_{*6}\eta^2\right]^{1/2}\left[1 - .75\, r\, \eta^2\right]^{1/2}\left(\gamma_1^2 - 1\right)^{1/2}} + \frac{\gamma_2}{\xi} \qquad (3.2.37)$$

where $j_{12} = j_* \times 10^{-12}$ and $R_{*6} = R_* \times 10^{-6}$. To simulate the fact that no acceleration takes place on the bounding field line ($\eta = \eta_{max}$) we shall replace j_{12} by $j_{12}(1-\eta^2/\eta_{max}^2)$ so that only a portion of the current causes acceleration.

The results of the integration are shown in figures 3 - 6 We note that the exact numerical results are completely consistent with the analytic approximate results. The initial behavior of δ with respect to δr is correct and there is, indeed, a maximum in the electric field at approximately $1.5R_*$.

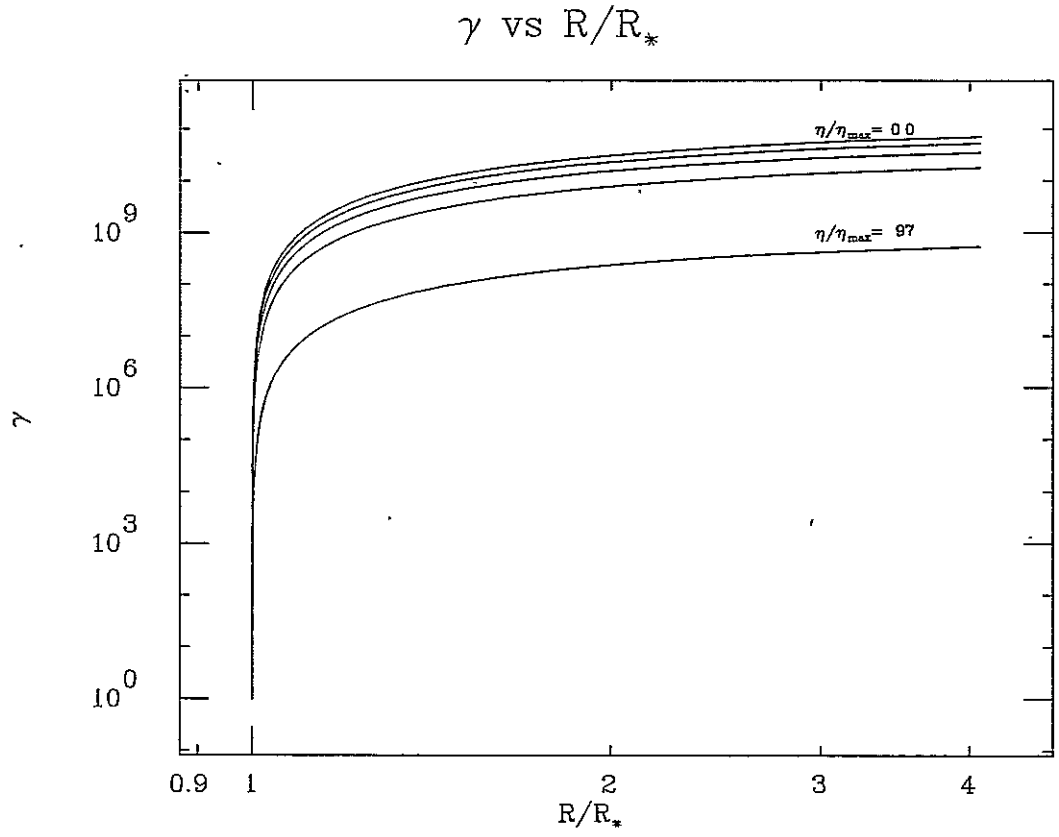

Figure 3: γ vs R/R_* for η/η_{max}= 0,.48,.69,.83,.97 and j_{12}=1. Values of η/η_{max} are plotted from top to bottom.

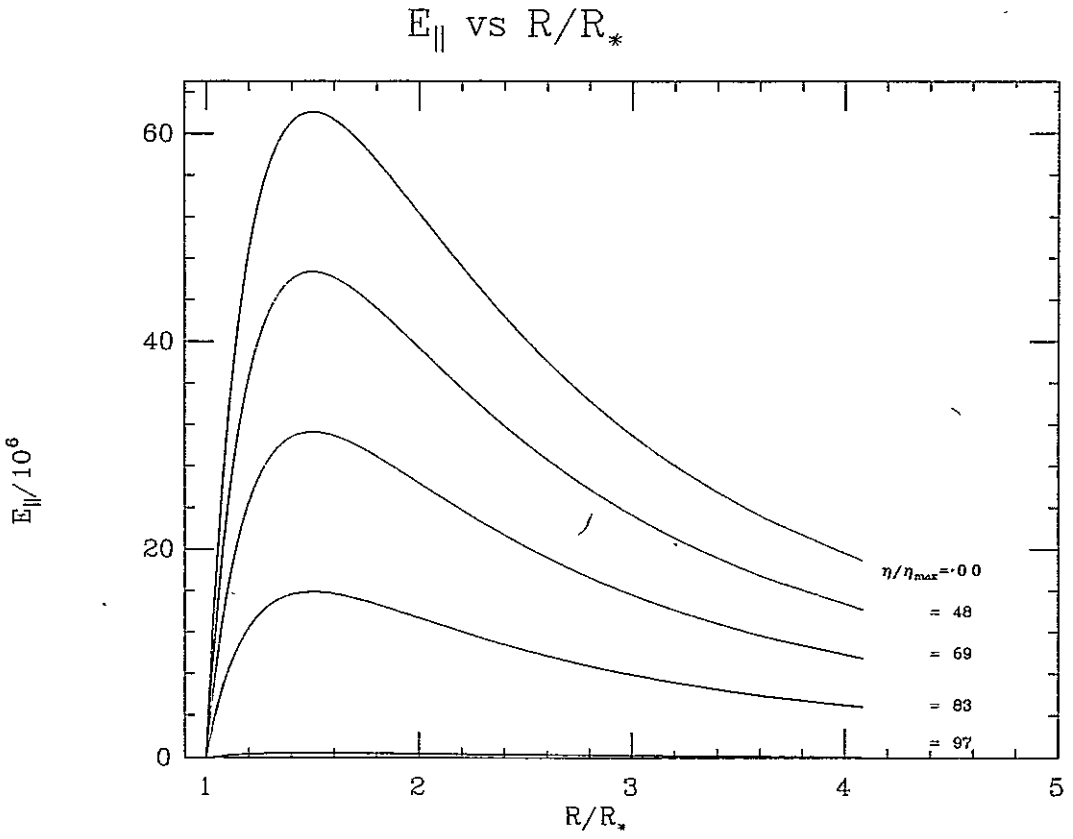

Figure 4: Accelerating electric field plotted vs. $r/R_\star$ for η/η_{max}=0,.48,.69,.83,..97 and j_{12}=1.

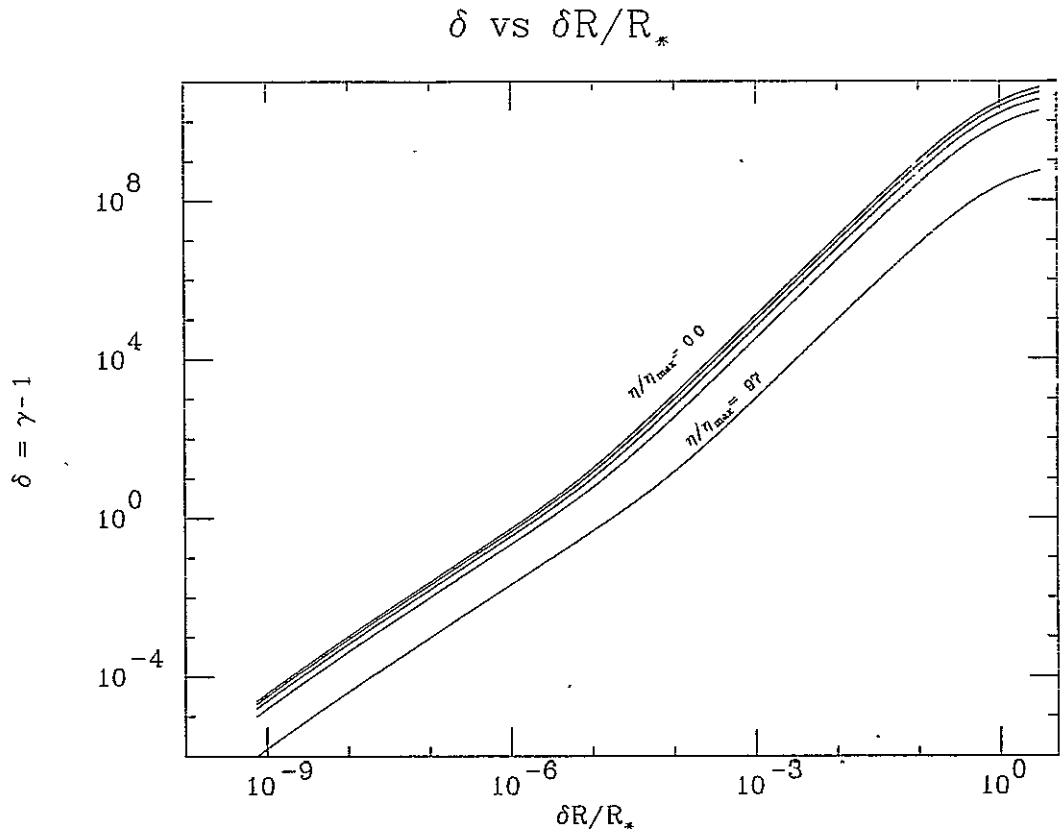

Figure 5: $\delta \equiv \gamma - 1$ plotted vs. $\delta r/R_*$ with η/η_{max}=0,.48,.69,.83,.97 and j_{12}=1.

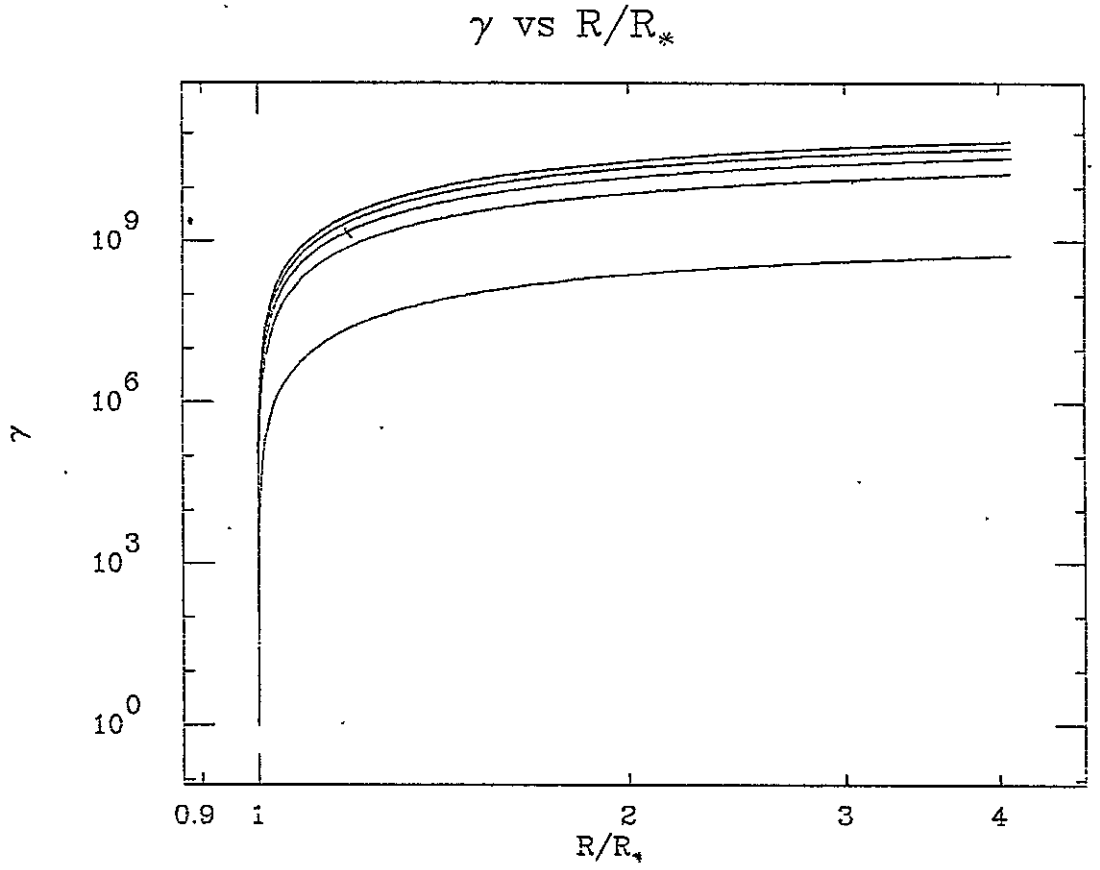

Figure 6: γ plotted for various values of j_*, with co-ordinate η=0. The values of j_{12} are: 1,.52,.31,.17,.03.

3.2.4 Two Dimensional Solution

We must now consider the two dimensional problem. It is certainly true that the time and ϕ dependence can be eliminated in the axisymmetric case, but it is probably a good approximation to use a two dimensional model even in the non-axisymmetric case. The two-dimensional problem is, however, much more difficult to work with than the one-dimensional case. In this section we will consider two different approaches to the problem. In the first method we shall assume a form for the transverse behavior of the electric potential and use a perturbation expansion in the co-ordinate η. The alternate approach is to assume that the current has the same η dependence as the potential and use a separation of variables technique.

3.2.4.1 Perturbation Method

We first analyse the two dimensional problem from the perturbation expansion approach. We know that the potential for the aligned rotator must be an even function of η so we expand it in a power series in η^2.

$$\Phi(\xi,\eta) = \sum a_i(\xi)\eta^{2i}/\eta_{max}^{2i} \qquad (3.2.38)$$

We also know that at the surface of the star the potential has the form $\Phi_*(1-\eta^2/\eta_{max}^2)$ which thus forms the boundary condition that the coeffiecients of all terms of order η^4 and higher must go to zero at the surface of the star, while a_1 must go to 1 (we may set a_0=1 without loss of generality). Finally, the condition that Φ = 0 at η_{max} requires

$$\sum_{i=1}^{\infty} a_i(\xi) = 1 \tag{3.2.39}$$

The basic assumption we need for a perturbation expansion is that $|a_i| < |a_{i-1}|$. Even with this assumption the problem involves a great deal of messy algebra. In working with the perturbation expansion, we must also expand j_* as a power series in η^2.

We now look at the problem to zeroth order in η. The potential must be expressed to first order and the current to zeroth order in η^2. We therefore set

$$\Phi = \Psi(\xi)(1-\eta^2/\eta^2_{max}) \tag{3.2.40}$$

Substituting equation (3.2.40) into equation (3.2.19) we find (to order η^2)

$$\frac{\left(1 - \frac{3}{4} r \eta^2\right)}{r^6 \xi}\left[\left(1 - \eta^2/\eta^2_{Max}\right) \frac{\partial}{\partial \xi}\left(\frac{1}{\xi} \frac{\partial \psi}{\partial \xi}\right) - \frac{4\psi \xi r^3}{\eta^2_{Max}} \left(1 - \frac{3}{4} r \eta^2\right)\right] \tag{3.2.41}$$

$$\simeq - \frac{4\pi j_0}{c} \left(\frac{R_*}{r}\right)^3 \left[1 - \frac{3}{8} r \eta^2 + \frac{3}{8} R_* \eta^2\right]$$

The zeroth order equation is then

$$\frac{1}{r^6 \xi} \frac{\partial}{\partial \xi}\left(\frac{1}{\xi} \frac{\partial \psi}{\partial \xi}\right) - \frac{4\psi}{r^3 \eta^2_{Max}} = - \frac{4\pi j_0}{c} \left(\frac{R_*}{r}\right)^3 \tag{3.2.42}$$

A particular solution to the inhomogeneous equation (3.2.42) is

$$\psi_p(\xi) = \frac{\pi j_0}{c} R_*^3 \eta^2_{Max} \tag{3.2.43}$$

The homogeneous equation may be written as

$$\xi \frac{\partial^2 \psi}{\partial \xi^2} - \frac{\partial \psi}{\partial \xi} - \frac{4\psi}{\eta_{Max}^2} = 0 \qquad (3.2.44)$$

To solve this equation we make the substitutions

$$u = \xi^{1/2} \quad \text{and} \quad \Psi(\xi) = u^2 Y(u) \qquad (3.2.45)$$

Equation (3.2.44) then becomes

$$\frac{d^2Y}{du^2} + \frac{1}{u}\frac{dY}{du} - \left[\frac{4}{u^2} + \frac{16}{\eta_{Max}^2}\right] Y = 0 \qquad (3.2.46)$$

This is the modified Bessels's equation of order 2 and parameter $4/\eta_{max}$. The solution to equation (3.2.42) is then given by

$$\psi(\xi) = c_1 \xi I_2 \left(\frac{4\sqrt{\xi}}{\eta_{Max}}\right) + c_2 \xi K_2 \left(\frac{4\sqrt{\xi}}{\eta_{Max}}\right) + \frac{\pi j_0}{c} R_*^3 \eta_{Max}^2 \qquad (3.2.47)$$

The boundary conditions at $r = R_y$ and $r = R_\star$ now determine the values of the constants. If $R_y \gg R_\star$ it is simpler to make the approximation that $\xi \simeq 0$ at the outer boundary. Then the I_2 term goes to zero and the remaining two terms must cancel. As $x \to 0$, $K_2(x) \to 2/x^2$ and we therefore find that

$$\frac{c_2}{8} \eta_{Max}^2 + \frac{\pi j_0}{c} R_*^3 \eta_{Max}^2 \simeq 0 \qquad (3.2.48)$$

and hence

$$c_2 \simeq - \frac{8\pi j_0 R_*^3}{c} \qquad (3.2.49)$$

At $\xi = 1/R_*$ we require

$$\psi(\xi_*) = -\frac{\Omega B_* R_*^3}{2c}\eta_{Max}^2 \qquad (3.2.50)$$

Since $4\xi^{1/2}/\eta_{max} >> 1$, we can use the asymptotic expansions of I_2 and K_2 to simplify equation (3.2.47) at the stellar surface.

$$I_2 \sim \frac{e^{\zeta}}{(2\pi\zeta)^{1/2}} \qquad \text{and} \qquad K_2 \sim \left(\frac{\pi}{2\zeta}\right)^{1/2} e^{-\zeta} \qquad (3.2.51)$$

where

$$\zeta = 4\xi^{1/2}/\eta_{max} \qquad (3.2.52)$$

Combining equations (3.2.49), (3.2.51), and (3.2.51) we then find

$$c_1 = -\left[\frac{\Omega B_*}{2} R_* \eta_{Max}^2 + \pi j_0 R_* \eta_{Max}^2 - 8\pi j_0 \left(\frac{\pi}{2\zeta_*}\right)^{1/2} e^{-\zeta_*}\right] \qquad (3.2.53)$$

$$\times \left[\frac{R_*^3}{c}(2\pi\zeta_*)^{1/2} e^{-\zeta_*}\right]$$

Finally, we require space-charge limited flow, which determines j_0. We write $d\Psi/d\xi$ in terms of ζ (as defined by equation 3.2.52)

$$\frac{d\psi}{d\xi} = \frac{8c_1}{\zeta\eta_{Max}^2}\frac{d}{d\zeta}\left[\frac{\zeta^2}{16}\eta_{Max}^2 I_2(\zeta)\right] + \frac{8c_2}{\zeta\eta_{Max}^2}\frac{d}{d\zeta}\left[\frac{\zeta^2}{16}\eta_{Max}^2 K_2(\zeta)\right] \qquad (3.2.54)$$

We also note that

$$\frac{d}{d\zeta}\left[\zeta^2 I_2(\zeta)\right] = \zeta^2 I_1(\zeta) \quad \text{and} \quad \frac{d}{d\zeta}\left[\zeta^2 K_2(\zeta)\right] = -\zeta^2 K_1(\zeta) \qquad (3.2.55)$$

Hence, at ξ_* we have

$$\left.\frac{d\psi}{d\xi}\right|_{\xi_*} = \frac{c_1}{2}\zeta_* I_1(\zeta_*) - \frac{c_2}{2}\zeta_* K_1(\zeta_*) = 0 \qquad (3.2.56)$$

and, combining equations (3.2.56) and (3.2.49) with the asymptotic expansions (equation 3.2.51), we get

$$c_1 = \pi\, e^{-2\zeta_*} \quad c_2 = -\frac{8\pi^2 j_0}{c} R_*^3\, e^{-2\zeta_*} \tag{3.2.57}$$

Finally, combining (3.2.57) and (3.2.53), we have

$$j_0 = \frac{\left(\frac{\zeta}{2\pi}\right)^{1/2} \Omega\, B_*\, R_*\, \eta_{Max}^2\, e^{\zeta}}{\left[16\pi - (2\pi\zeta)^{1/2} e^{\zeta}\, R_*\, \eta_{Max}^2\right]} \simeq -\frac{\Omega\, B_*}{2\pi} \tag{3.2.58}$$

which is the value of j_* originally estimated by Sturrock (1971) and the value of j which gives the G-J charge density at the surface.

One of the original motives for analyzing dipole field lines was to get large acceleration near the stellar surface. However, the zeroth order solution for the aligned rotator does not produce significant acceleration. Actually, this is to be expected, since at this order we have only included corrections of order θ^2 and we have simply recovered the G-J charged density in a region where the field lines are very nearly straight (see the theorem described in section 1.1 of this chapter). We must therefore extend the analysis to second order in η in order to determine what acceleration (if any) is produced near the surface. We set

$$\Phi = \psi(\xi)\left[1 - \eta^2/\eta_{Max}^2 + G_2(\xi)\,\eta^2/\eta_{Max}^2 - G_2(\xi)\,\eta^4/\eta_{Max}^4\right] \tag{3.2.59}$$

$$j_* = j_0\left(1 + b\,\eta^2/\eta_{Max}^2\right)$$

and we note that a_2 is a function of ξ but b is a constant. Substituting into equation (3.2.19) we now find the zeroth order

equation is

$$\xi^2\left[\frac{\partial}{\partial\xi}\left(\frac{1}{\xi}\frac{\partial\psi}{\partial\xi}\right)-\frac{4\psi}{\xi^2\eta_{Max}^2}+\frac{4\psi G_2}{\xi^2\eta_{Max}^2}\right]=-\frac{4\pi j_0 R_*^3}{c} \qquad (3.2.60)$$

while the second order equation is

$$\xi^2\left\{-\frac{\partial}{\partial\xi}\left(\frac{1}{\xi}\frac{\partial\psi}{\partial\xi}\right)\frac{1}{\eta_{Max}^2}+\left[\frac{G_2}{\xi}\frac{\partial^2\psi}{\partial\xi^2}-\frac{G_2}{\xi^2}\frac{\partial\psi}{\partial\xi}+\frac{2}{\xi}\frac{\partial\psi}{\partial\xi}\frac{\partial G_2}{\partial\xi}\right.\right.$$

$$\left.\left.-\frac{\psi}{\xi^2}\frac{\partial G_2}{\partial\xi}+\frac{\psi}{\xi}\frac{\partial^2 G_2}{\partial\xi^2}\right]\frac{1}{\eta_{Max}^2}-\frac{\partial\psi G_2}{\xi^2\eta_{Max}^2}\left(\frac{3}{\xi}-\frac{8}{\eta_{Max}^2}\right)\right\} \qquad (3.2.61)$$

$$=-\frac{4\pi j_0 R_*^3}{c}\left[-\frac{3}{8}\frac{1}{\xi}+\frac{3}{8}R_*+\frac{b}{\eta_{Max}^2}\right]$$

We note that the zeroth order equation has been modified from equation (3.2.42) but we are assumming that $a_2 << 1$ so to solve these equations we first set $a_2 = 0$ in equation (3.2.60) (thus recovering the original zeroth order solutions equation (3.2.47)) and then use that solution in equation (3.2.61) to eliminate the Ψ dependence. To solve equation (3.2.61), we first define a new variable

$$\beta = \Psi a_2/\xi \qquad (3.2.62)$$

With this definition and using equation (3.2.60), equation (3.2.61) can be rewritten as

$$\left[\xi^2\frac{\partial^2\beta}{\partial\xi^2}+\xi\frac{\partial\beta}{\partial\xi}-\beta\right]\frac{1}{\eta_{Max}^2}-\frac{2\xi}{\eta_{Max}^2}\left(\frac{3}{\xi}-\frac{8}{\eta_{Max}^2}\right)\beta \qquad (3.2.63)$$

$$=\xi^2\frac{\partial}{\partial\xi}\left(\frac{1}{\xi}\frac{\partial\psi}{\partial\xi}\right)\frac{1}{\eta_{Max}^2}-\frac{4\pi j_0 R_*^3}{c}\left[-\frac{3}{8\xi}+\frac{3}{8}R_*+\frac{b}{\eta_{Max}^2}\right]$$

We again change the independent variable to $u^2=\xi$ and find

$$u^2 \frac{d^2\beta}{du^2} + u \frac{d\beta}{du} + \left(\frac{64u^2}{\eta_{Max}^2} - 28 \right) \beta$$

$$= - \frac{4\pi j_0 R_*^3}{c} \left[- \frac{3}{8u^2} + \frac{3}{8} R_* + \frac{b+1}{\eta_{Max}^2} \right] \eta_{Max}^2 + \frac{4\psi}{\eta_{Max}^2} \qquad (3.2.64)$$

The boundary condition for β at the surface is clearly $\beta(u_*)=0$. (Since $a_2=0$ at the surface.) At the outer surface the condition becomes $\beta u^2 \to 0$ as $u \to 0$. This is true as long as a_2 does not blow up at $\xi=0$. While this leaves β undetermined on the outer boundary, we shall require the stronger condition $\beta=0$ at $u=0$. The condition of space-charge limited flow requires

$$\frac{d}{d\xi} (\beta\xi) \Big|_{\xi_*} = \beta + \xi \frac{d\beta}{d\xi} \Big|_{\xi_*} = \beta - \frac{u}{2} \frac{d\beta}{du} \Big|_{u_*} = 0 \qquad (3.2.65)$$

Since β itself is also 0 at $u = u_*$ we then have $d\beta/du = 0$ at u_*.

We can immediately determine the constant "b" in equation (3.2.59).. At u_* equation (3.2.64) reduces to

$$- \frac{4\pi j_0 R_*^3}{c} (b+1) + \frac{4\psi(\xi_*)}{\eta_{Max}^2} = 0 \qquad (3.2.66)$$

and thus "b" is given by

$$b = \frac{4\psi(\xi_*)}{\eta_{Max}^2} \frac{c}{4\pi j_0 R_*^3} - 1 \qquad (3.2.67)$$

Substituting from equations (3.2.58) and (3.2.50), we immediately find that $b\equiv 0$. Thus there is no second order correction to the current. To solve equation (3.2.64) we use a Green function approach. The Green

unction for this equation (Bessel's equation) is given by (see Appendix
for details)

$$G(u,u') = \frac{\pi}{2a} J_\alpha(\lambda u_<)\left[J_\alpha(\lambda u_>) + aN_\alpha(\lambda u_>)\right] \qquad (3.2.68)$$

here

$$\alpha = \sqrt{28} \qquad (3.2.69)$$

nd

$$\lambda = 8/\eta_{max} \qquad (3.2.70)$$

$$a = -J_\alpha(\lambda u_*)/N_\alpha(\lambda u_*) \qquad (3.2.71)$$

Thus the solution to equation (3.2.64), with β=0 on the boundaries, is given by

$$\beta(u) = -\frac{4\pi j_0 R_*^3 \eta_{Max}^2}{c}\int_0^{u_*} G(u,u')\left[-\frac{3}{8u'^2} + \frac{3}{8}R_* + \frac{1}{\eta_{Max}^2} + \frac{4\psi}{\eta_{Max}^2}\right]du' \qquad (3.2.72)$$

Explicitly substituting (3.2.68) into this equation we find the formal

solution

$$\beta(u) = -\frac{4\pi j_0 R_*^3}{c}\ \frac{\pi}{2a}\left\{\left[\frac{3}{8}R_* + \frac{1}{\eta_{Max}^2}\right]\ \times\right.$$

$$\left[J_\alpha(\lambda u)\int_0^{u_*} J_\alpha(\lambda u')du' + a\,N_\alpha(\lambda u)\int_0^{u} J_\alpha(\lambda u')du'\right.$$

$$\left. + a\,J_\alpha(\lambda u)\int_u^{u_*} N_\alpha(\lambda u')du'\right]$$

$$- \frac{3}{8}\left[J_\alpha(\lambda u)\int_0^{u_*} \frac{J_\alpha(\lambda u')}{u'^2}\,du' + a\,N_\alpha(\lambda u)\int_0^{u} \frac{J_\alpha(\lambda u')}{u'^2}\,du'\right. \qquad (3.2.73)$$

$$\left. + a\,J_\alpha(\lambda u)\int_u^{u_*} \frac{N_\alpha(\lambda u')}{u'^2}\,du'\right]$$

$$+ \frac{4}{\eta_{Max}^2}\left[J_\alpha(\lambda u)\int_0^{u_*} \psi(u'^2)J_\alpha(\lambda u')du' + a\,J_\alpha(\lambda u)\int_u^{u_*} \psi(u'^2)N_\alpha(\lambda u')du'\right.$$

$$\left.\left. + a\,N_\alpha(\lambda u)\int_0^{u} \psi(u'^2)J_\alpha(\lambda u')du'\right]\right\}$$

3.2.4.2 Separation of Variables Method

In this method we look for solutions to equation (3.2.19) in which the η dependence of Φ is the same as that of j_*. We further assume that Φ and j_* can be written as

$$\Phi(\xi,\eta) = \Psi(\xi)H(\eta) \tag{3.2.74}$$

$$j_*(\eta) = j_0 H(\eta) \tag{3.2.75}$$

We note, however, that equation (3.2.19) is clearly not separable in these co-ordinates and we must therefore approximate it in order to render it separable. We write equation (3.2.19) to lowest order in η to get

$$\xi^2 \frac{\partial}{\partial\xi}\left(\frac{1}{\xi}\frac{\partial\Phi}{\partial\xi}\right) + \frac{1}{\eta}\frac{\partial}{\partial\eta}\left(\eta\frac{\partial\Phi}{\partial\eta}\right) = -\frac{4\pi j_*(\eta)}{c} R_*^3 \tag{3.2.76}$$

We now substitute equations (3.2.74) and (3.2.75) into (3.2.76).

$$\xi\,\psi''H - \psi'H + \psi H'' + \frac{1}{\eta}\psi H' = -\frac{4\pi j_0}{c} R_*^3 H \tag{3.2.77}$$

Dividing by ΨH and regrouping terms gives us

$$\frac{\xi\psi''}{\psi} - \frac{\psi''}{\psi} + \frac{4\pi j_0 R_*^3}{c\psi} = -\left(\frac{H''}{H} + \frac{H''}{\eta H}\right) \tag{3.2.78}$$

The left hand side of equation (3.2.78) is a function of ξ only, while the right hand side is a function of η only. We therefore have the two equations

$$\xi\psi'' - \psi' - \alpha^2\psi = -\frac{4\pi j_0 R_*^3}{c} \tag{3.2.79}$$

and

$$H'' + \frac{1}{\eta} H' + \alpha^2 H = 0 \tag{3.2.80}$$

The solution to equation (3.2.80) is then given by the J_0 Bessel function.

$$H(\eta) = J_0(\alpha\eta) \tag{3.2.81}$$

Equation (3.2.79) will be recognized as identical in form to equation (3.2.42) and we can therefore immediately write down the solution to equation (3.2.79) as

$$\psi(\xi) = c_1 \xi I_2\left(\alpha\sqrt{\xi}\right) + c_2\,\xi\, K_2\left(\alpha\sqrt{\xi}\right) + \frac{4\pi j_0}{\alpha^2 c} R_*^3 \tag{3.2.82}$$

The boundary condition on closed field lines requires

$$J_0(\alpha\eta_{max}) = 0 \tag{3.2.83}$$

Thus the separation constant α is determined by the zeros of J_0.

The only remaining task is to evaluate constants. The potential may now be expressed in the following form:

$$\Phi(\xi,\eta) = \sum_{i=1}^{\infty} \left[c_{1i}\,\xi I_2\left(\chi_i \frac{\sqrt{\xi}}{\eta_{Max}}\right) + c_{2i}\xi K_2\left(\chi_i \frac{\sqrt{\xi}}{\eta_{Max}}\right) + \frac{4\pi j_i}{\chi_i^2\, c} R_*^3\, \eta_{Max}^2 \right] J_0\left(\chi_i\, \eta/\eta_{Max}\right) \tag{3.2.84}$$

where χ_i is the i^{th} zero of J_0. Following the same lines as in the perturbation method (see equations (3.2.49) - (3.2.58)) and using the orthogonality properties of the Bessel functions, we find that the

constants are given by

$$c_{2i} = - \frac{32\pi\, j_i\, R_*^3}{\chi_i^2\, c} \tag{3.2.85}$$

$$c_{1i} = - \frac{32\pi^2\, j_i\, R_*^3}{\chi_i^2\, c}\; e^{- \frac{2\chi_i \sqrt{\xi_*}}{\eta_{Max}}} \tag{3.2.86}$$

The requirement of space-charge limited flow then determines the j_i's.

$$j_i \simeq - \frac{\Omega\, B_*}{\pi\, \chi_i\, J_1(\chi_i)} \tag{3.2.87}$$

and the total current is given by

$$j_*(\eta) = - \frac{\Omega\, B_*}{\pi} \sum_{i=1}^{\infty} \frac{J_0(\chi_i\, \eta/\eta_{Max})}{\chi_i\, J_1(\chi_i)} \tag{3.2.88}$$

Chapter IV

DISCUSSION AND CONCLUSION

4.1 THE ACCELERATION PROBLEM

4.1.1 The charge separated model

As is clear from the preceding chapter, the exact mechanism by which charged particles are accelerated is still a problem. Fundamentally this is due to our lack of knowledge about conditions in the outer magnetosphere (near the light cylinder, or perhaps near R_{FB}). We know that at the light cylinder, the field lines must "slip" through the plasma or be highly distorted. If this were not true no EMF could be generated. An additional complication comes from the requirement that acceleration take place near the surface of the star (this is required in polar-cap emission models) and that of space-charge limited flow. The space-charge limited flow produces zero acceleration at the surface and the slow change of the angle between $\underset{\sim}{\Omega}$ and $\underset{\sim}{B}$ means that only a very small accelerating electric field can develop near the surface. In the context of a model with dipole field lines, it seems that we must either abandon space-charge limited flow or the requirement that acceleration take place near the surface. Larger acceleration will occur near the stellar surface, however, if the magnetic field lines near the surface curve more rapidly than in the dipole case.

The latter of these two choices is the more attractive. Referring again to figure 2 in Chapter II we note that the data indicate that the

polar cap is larger than estimated in the PCLC models. In the PCFB model, the polar cap was made large by moving the point R_y from the light cylinder to the force balance radius. An alternate approach, however, would be to move the radiation producing region out from the stellar surface. The fanning out of the magnetic field lines would then produce a wider beam. If this is the correct solution, the data suggest that the emission region is at a significantly larger distance from the surface than previously suggested in polar-cap models.

A simple linear least-squares fit to the data shown in figure 2 gives the following formula for the pulse width for a given period:

$$\log(W) = 1.43 + 0.70 \times \log(P) \qquad (4.1.1)$$

where W is measured in milliseconds and P in seconds. It is impossible to confirm the slope, however, since there is a range of slopes which give a good fit provided the constant term is chosen right. In comparing the fit for a slope of $\frac{1}{2}$ (PCLC) with the fit for a slope of 2/3 (PCFB), we find there is no significant improvement. The least-squares fit for a slope of $\frac{1}{2}$ gives a constant term of 1.40. The width of the emission cone (in seconds) for emission occurring at a distance r_e from the center is given by

$$W = \frac{3}{2}\left(\frac{r_e}{R_y}\right)^{1/2} \frac{P}{\pi} \qquad (4.1.2)$$

The least-squares fit then suggests that the emission region is located approximately at $r_e \sim 50R_*$.

Another difficulty in analyzing the acceleration mechanism is due to the nature of the curved field lines. We know that we must have curved field lines in order to get acceleration, but the most realistic case

(dipole field) is very difficult to work with because Laplace's equation is not separable. Small angle approximations are possible (as was done in the final section of Chapter III), but the method is not valid for large distances, which appears to be an important region for the physics of the problem. A possible solution to this difficulty is to use some co-ordinate system which is separable and still mimics the general morphology of the dipole field lines. One such co-ordinate system is that of "toroidal" co-ordinates. Laplace's equation is separable (although the Helmholz equation is not) and the "field lines" in this system would curve in the same direction as the dipole field lines, meeting the equatorial plane at right angles to the plane (as do dipole field lines). The radius of curvature is, however, much shorter than the dipole case which would probably produce excessively high acceleration. The method might be useful, nevertheless, as an indication of when acceleration can be expected and perhaps might serve as an upper bound on how much acceleration can be expected.

4.1.2 The effects of pair production

As noted at the beginning of Chapter III, it is important that the plasma be charge separated. Thus, either pair production must not take place, or the effects of pair production must be negligible in order for the equations to be valid. If pair production does take place, there are several effects on the equations. First, the current is no longer tied to the magnetic field lines, since a particle may produce a gamma ray via the curvature radiation mechanism, which then crosses field lines until it produces an electron-positron pair on a new field line.

Thus current can be transported across field lines even if individual articles are firmly attached to the field lines. A second effect is hat the charge density may no longer be simply related to the current ensity. Indeed, once pair production takes place, the number of pairs xpected is large, so in order for the charge-separated equations to till be valid, the velocity difference between electrons and positrons ust be extremely small. Since, however, the electrons and positrons ill be accelerated in opposite directions (if the accelerating field is non-zero), it is unreasonable to expect the velocity difference to remain small even if the initial difference is negligible. We would then expect the electron-positron plasma to distribute itself so as to shield the particles from the accelerating field. Thus, once pairs are produced, the acceleration will be sharply reduced. This might not affect the radio emission process (in fact it may be the source of the radio emission mechanism, e.g. the beam-plasma instability postulated in the Ruderman-Sutherland model), but the decreased acceleration makes it difficult to account for the high-energy gamma rays that have been observed from the Crab pulsar (Ogelman, et al. 1976).

4.1.3 The effects of particle inertia

One of the results of the acceleration theorem presented in Chapter III is to suggest that the effect of particle mass is even more important that previously realized. It has long been suggested that the accelerated particles would tend to wrap up the magnetic field lines when inertial effects became important compared to electro-magnetic effects. Since it is now clear that such distortions of the magnetic

field are accompanied by accelerating electric fields, it is important to consider the particle masses in explaining the acceleration mechanism. The analysis of the problem with particle masses included is extremely complicated and will probably require detailed computer modeling in order to solve the equations.

4.1.4 Return currents: Is a pulsar charged?

In the polar-cap region, particles of only one sign are accelerated, and the same particles are accelerated from both poles. It is clear that the accelerated particles cannot be accelerated indefinitely and removed from the pulsar, or the pulsar would quickly develop a charge sufficient to turn off the current. Either particles of both signs must be removed from the surface (an unlikely situation except in the orthogonal rotator case, see Chapter II - Holloway's analysis) or there must be a deceleration region in which the particles are slowed down and transported to other field lines in the closed field region and returned to the star. One would suspect that particles cross field lines when $|E| > |B|$. If the star has a net charge, Q, and we ignore the co-rotation E field, the particles would be expected to cross field lines when

$$\frac{Q}{r^2} \geq B_* \left(\frac{R_*}{r}\right)^3 \qquad (4.1.3)$$

If we then demand that particles cross field lines at R_L we can solve for Q to find

$$Q \sim \Omega B_* R_*^3/c \qquad (4.1.4)$$

In fact, this large a charge on the star itself would be sufficient to

stop the acceleration of particles entirely and ultimately leave a vacuum around the pulsar (Jackson, 1976). Presumably then a smaller net charge appropriately distributed in the magnetosphere, along with the rotational electric field is sufficient to make the accelerated particles cross field lines. By dealing with a vacuum "magnetosphere", Jackson (1976) has estimated the charge on the star to be a third of the above value. In fact, if the charge imbalance is distributed near the "Y-type neutral point" rather than on the star itself (as is likely), the charge imbalance may be significantly less than either estimate. In any case, it is quite likely that a charge imbalance is present and that it forces the accelerated particles to cross magnetic field lines and return to the neutron star along the closed field lines.

4.2 THE RADIATION PROBLEM

While the radio emission of pulsars seems to fit a fairly simple conceptual model (although the details of the emission mechanism are not well understood), the other forms of radiation present a bewildering variety of properties. Two pulsars, the Crab and the Vela pulsars, have been detected optically. The Crab pulsar has also been detected in the infrared and the x-ray region (Cocke, et al. 1969; Wallace, et al. 1977). Gamma radiation has been detected from four pulsars (PSR-0532[the Crab], PSR-0833[the Vela], PSR-1747, and PSR-1818)(Thompson, et al. 1975; Buccheri, et al. 1976; Ogelman, et al. 1976). In the case of the Crab pulsar the gamma ray energies are known to exceed 1 Gev. All the pulsed radiation of the Crab pulsar (except to extremely high-energy gamma rays ~ 10^{12} eV) is in phase with the

principal radio pulses. In the case of the Vela pulsar, there is only one radio pulse, but two optical pulses and two gamma ray pulses, none of which is in phase with any of the others. For PSR-1747 and PSR-1818. there is one radio pulse and one gamma ray pulse but in neither case are the two in phase. Table 4 summarizes the situation and the relative phases.

TABLE 4

Relative Phases of Radio, Optical, X-Ray, and Gamm Ray Pulses for four pulsars.

Pulsar	Phase				
	radio	optical	x-ray	gamma ray	very energetic gamma rays
0532 (Crab)	-20° (precursor) 0° (main pulse) 143° (interpulse)	 0° 143°	 0° 143°	 0° 143°	variable
0833 (Vela)	0°	100° 196°		60° 223°	
1747-46	0°			57°	
1818-04	0°			263°	

It is unlikely that any simple model can explain such a diversity of facts. The fact that radiation occurs at phases other than those which we would ascribe to the polar caps (i.e. the phase of the radio pulse), indicates that some of the radiation occurs elsewhere in the magnetosphere. This is also supported by the fact that high-energy gamma rays produced at the polar cap would be eliminated by the pair-production process. The Crab pulsar then appears to be anomalous in the

fact that pulses at all wavelengths are in phase. It is quite possible hat the Crab pulsar is the one pulsar in which we observe radio mission from the light cylinder (or force balance) region. In that ase, all the radiation from the Crab is produced in one area in the uter magnetosphere with the possible exception of the precursor. In act, the precursor may be the polar-cap radio pulse that we observe in ll other pulsars. The fact that two pulses symmetrically arranged bout a center phase are observed in both the Crab and the Vela pulsars (for both optical and gamma ray radiation) suggests that this radiation is occuring in the outer magnetosphere where the opening angle of the open field line region is large. If this is the case, the resultant radiation pattern is closer to a "fan beam" than to a "pencil beam", thus explaining why we see both pulses in both the Vela and Crab pulsars.

4.3 CONCLUSION

To paraphrase (and invert) Voltaire's famous aphorism about God, if pulsars did not exist, it would not be necessary to invent them. Indeed, based on our current theoretical understanding of pulsars, the fact of their existence seems quite remarkable. Nevertheless, we can come to a few conclusions:

1. If the magnetic field lines are curved (as they will be in any realistic model), particle acceleration (or deceleration) must occur.

2. If we assume space-charge limited flow, the acceleration does not occur near the surface of the star, but rather it occurs at distances of the order of a few to hundreds of star radii from the surface.

3. It is likely that the star-magnetosphere system has a net charge, the effect of which is to force particles emitted from the polar-cap region to cross magnetic field lines and eventually return to the star. Thus closed current loops are present and the system is in a (quasi) steady state.

There is clearly much work yet to be done to establish a clear understanding of pulsars. Primarily we need to understand the structure of the magnetosphere near the light cylinder where particle inertia becomes important. Once we finally understand the magnetosphere, it will be possible to construct believable radiation emission mechanisms. Once the plasma processes are understood we will finally be able to make a strict comparison between the theoretical models and the observed radiation.

It is implicit in the nature of an astrophysicist to be optimistic about the possibilities of understanding the distant and mysterious objects in the heavens. So the work on pulsar models will go on and better models will be produced. The task remains a difficult one and it is perhaps unfortunate that the LGM theory had to be dispensed with. Viewed in the light of what we know today it had many attractive features.

Appendix A

MATHEMATICAL DETAILS

A.1 GREEN FUNCTION FOR THE SECOND ORDER PERTURBATION

The Green function for equation (3.2.64) can be easily expressed in terms of the solutions to the homogeneous equation. The equation is Bessel's equation of order $\alpha = \sqrt{28}$ and parameter $\lambda = 8/\eta_{max}$. We wish to form a Green function for the interval $0 \le u \le u_*$ satisfying homogeneous boundary conditions. For $u<u'$ we want $G(0,u')=0$. For $u>u'$ we need $G(u_*,u')=0$. We therefore write G as follows:

$$G(u,u') = c\, J_\alpha(\lambda u_<)\left[J_\alpha(\lambda u_>) + a\, N_\alpha(\lambda u_>)\right] \tag{A.1}$$

where $u_< = \min(u,u')$ and $u_> = \max(u,u')$. At the point $u=u'$ there is a discontinuity in the first derivative given by

$$\left.\frac{dG(u,u')}{du}\right|_+ - \left.\frac{dG(u,u')}{du}\right|_- = \frac{1}{u'} \tag{A.2}$$

but we also know that the derivative discontinuity is given by

$$Ca\lambda W(J_\alpha, N_\alpha) \tag{A.3}$$

where W is the Wronskian of J_α and N_α evaluated at the point u. The Wronskian is given by (Cf. Stegun and Abramowitz, eqn. 9.1.16)

$$W(J_\alpha, N_\alpha) = 2/(\pi\lambda u) \tag{A.4}$$

It immediately follows that the normalization constant 'C' is given by

$$C = \pi/2a \tag{A.5}$$

Finally, the value of 'a' is determined by the boundary condition

$\mathcal{J}(u_*,u')=0$, which implies

$$a = -J_\alpha(\lambda u_*)/N_\alpha(\lambda u_*) \tag{A.6}$$

A.2 EXACT INTEGRATION OF THE NON-LINEAR PROBLEM

We start from equation (3.2.7) (repeated here for convenience)

$$\frac{d\gamma}{dr} = \left[\frac{8\pi e j_*}{m_0 c^3}\right]^{1/2} \left(\frac{R_*}{r}\right)^{3/2} (\gamma^2-1)^{1/4} \tag{A.7}$$

We now make the substitution $\cosh y = \gamma$. Equation (A.7) then can be written as

$$\sinh y \frac{dy}{dr} = K \left(\frac{R_*}{r}\right)^{3/2} (\sinh y)^{1/2} \tag{A.8}$$

where

$$K = \left(\frac{8\pi e j_*}{m_0 c^3}\right)^{1/2} \tag{A.9}$$

and we may therefore integrate both sides to find

$$\int_0^y (\sinh y')^{1/2}\, dy' = K\, R_*^{3/2} \int_{R_*}^r r^{-3/2}\, dr \tag{A.10}$$

The right hand side is trivial in integrate; the left hand side can be found in Gradshten and Ryzhik (1965) [equation 2.464.5 pg. 115] with the result given in equation (3.2.9).

Appendix B

COMPUTER LISTINGS

The following are listings of the programs and subroutines that were d in the numerical solution to the non-linear one-dimensional ation (see Chapter III, section 2.3). The subroutine "ODE" and its support routine "DE" were written by Shampine and Gordon. All routines except one are written in IBM Fortran IV (level H). The one exception, the subroutine "INVRT" was written in the IBM 370 assembly language.

```
C
C     PROGRAM TO SOLVE THE NON-LINEAR ONE-DIMENSIONAL DIFFERENTIAL EQUATION
C     WHICH DESCRIBES THE ACCELERATION OF CHARGED PARTICLES FROM THE POLAR CAP OF A
C
      IMPLICIT REAL*8 (A-H,O-Z)
      REAL*8 GAM(2),WORK(150)
      INTEGER IWORK(5)
      COMMON ZKAPPA,ETA,ETA2
      EXTERNAL F
C
C     VARIABLES USED:
C           P = PERIOD
C           B = SURFACE MAGNETIC FIELD
C           RSTAR = RADIUS OF THE STAR IN CM
C           ETAMAX = MAXIMUM VALUE OF THE CO-ORDINATE ETA
C           ETAMX2 = ETAMAX**2
C           GAM(1) = RELATIVISTIC GAMMA
C           GAM(2) = D(GAMMA)/D(XI)
C           XJSTAR = CURRENT DENSITY*1.0E-12*(1.-ETA**2/ETAMX2)
C           EPSI = ACCELERATING ELECTRIC FIELD*1.0E-6
C
C
C     ASSUME P=1 SEC
C     B=10**12 GAUSS
C
      RSTAR=1.0D+6
      ETAMX2=2.0*3.1415927/3.0D+10
      DETA=ETAMX2/129.
      ZKAP0=2.459D17
```

```
      ABSERR=0.0
      RELERR=1.0D-6

      DO 10 I=1,129,32
      ETA2=(I-1)*DETA
      ETA=DSQRT(ETA2)
      ZKAPPA=ZKAP0/DSQRT(1.0D0-.75D6*ETA2)*(1.0D0-ETA2/ETAMX2)
      XJSTAR=1.0D0-ETA2/ETAMX2
      GAM(1)=1.0D0+2.59D-6*XJSTAR**(2.0D0/3.0D0)
      GAM(2)=-1.6D+9*(1.0D0+2.0D-10)*XJSTAR**(2.0D0/3.0D0)
      PSI0=DSQRT(DSQRT(1.0D0-1.0D6*ETA2))*1.0D-6
      WRITE(6,110)ETA,ZKAPPA,XJSTAR
  110 FORMAT('1INTEGRATION FOR ETA = ',F12.6,10X,'KAPPA ='
     &,1PD20.12,5X,'JSTAR =',F10.6/8X,'PSI',12X,'RADIUS',9X,'DELTA-R'
     @,8X,'GAMMA',10X,
     *'DGAMMA',7X,'LOG(GAMMA)',7X,'E-PSI',7X,'IFLAG'/)
      PSIMAX=.25*PSI0
      PSTEP=(PSIMAX-PSI0)*1.0D-9
      PSMAX=(PSIMAX-PSI0)/50.D0
      CALL INVRT(PSI0,ETA,R,SN,CSN)
      DR=1.0
      GLOG=DLOG10(GAM(1))
      DELTA=1.0D-4/RSTAR
      GDELT=GAM(1)-1.0D0
      EPSI=-851.67D-6*DSQRT(1.0D0+3.0D0*CSN)/R**3/PSI0*GAM(2)
      WRITE(6,100)PSI0,DR,DELTA,GAM(1),GDELT,GLOG,EPSI
      WRITE(9,103)DR,GAM(1)
      WRITE(10,103)DR,EPSI
      WRITE(11,103)DELTA,GDELT
  103 FORMAT(1X,2D20.12)
  100 FORMAT(1P7D15.7,5X,I5)
      POUT=PSI0
      PSI=PSI0
      IFLAG=1
      DO 15 J=1,1000
      POUT=PSI+PSTEP
      CALL ODE(F,2,GAM,PSI,POUT,RELERR,ABSERR,IFLAG,WORK,IWORK)
      GLOG=DLOG10(GAM(1))
      GDELT=GAM(1)-1.0D0
      IF(IFLAG.LT.0)GO TO 16
      CALL INVRT(PSI,ETA,R,SN,CSN)
      DR=R/RSTAR
      DELTA=(R-RSTAR)/RSTAR
      EPSI=-851.67D-6*DSQRT(1.0D0+3.0D0*CSN)/R**3/PSI*GAM(2)
      WRITE(6,100)PSI,DR,DELTA,GAM(1),GDELT,GLOG,EPSI,IFLAG
      WRITE(9,103)DR,GAM(1)
      WRITE(10,103)DR,EPSI
      WRITE(11,103)DELTA,GDELT
      GO TO 18
   16 WRITE(6,101)IFLAG,PSI,POUT
  101 FORMAT('0***ERROR:  IFLAG=',I4,10X,1P2D20.12)
      STOP
   18 IF(PSMAX.LE.PSTEP)PSTEP=PSTEP+PSTEP
      IF(PSI.LT.PSIMAX)GO TO 11
```

```
   15 CONTINUE

      OUTPUT DATA FOR LATER PLOTTING USING 'TOP DRAWER'

   11 WRITE(9,104)
      WRITE(10,104)
      WRITE(11,104)
  104 FORMAT(1X,'JOIN')
   10 CONTINUE
      STOP
      END
      SUBROUTINE F(PSI,GAM,DGAM)

      THIS SUBROUTINE IS USED BY ODE
      IT DEFINES THE DIFFERENTIAL EQUATION TO BE INTEGRATED

      IMPLICIT REAL*8(A-H,O-Z)
      REAL*8 GAM(2),DGAM(2)
      COMMON ZKAPPA,ETA,ETA2
      DGAM(1)=GAM(2)
      CALL INVRT(PSI,ETA,R,SN,CSN)
      DGAM(2)=ZKAPPA*R**3*PSI**2/DSQRT(1.0D0-.75D0*R*ETA2)*GAM(1)/
     &DSQRT(GAM(1)**2-1.0D0)+GAM(2)/PSI
      RETURN
      END
```

Subroutine "INVRT" is used to convert values of η and ξ to values of r and θ. It uses Newton's method to solve first for the value of r and then determines $\sin^2(\theta)$ and $\cos^2(\theta)$ from the definitions of η and ξ.

```
*
*        SUBROUTINE INVRT(PSI,ETA,R,SN,CSN)
*
INVRT    START
         USING *,15
         B     START
         DC X'5',CL7'INVRT
*
SAV      DS 18F
*
START    EQU *
         STM 14,12,12(13)    SAV REGS
         ST 13,SAV+4         SAVE ADDRESS OM MY SAV AREA
```

```
         LA 12,SAV           LOAD ADDRESS OF MY SAVE AREA
         ST 12,8(13)         STORE IN CALLING SAVE AREA
         LR 13,12            MAKE 13 THE BASE REG.
         DROP 15
         USING SAV,13
         LM 2,6,0(1)         LOAD ARGUMENT ADRESSES
         LD 0,0(3)           LOAD ETA
         LTDR 0,0            TEST ETA
         BZ ZERO             IF 0 GO TO ZERO
         MDR 0,0             SQUARE ETA
         STD 0,ETA           SAVE ETA**2
         LD 2,0(2)           LOAD PSI
         STD 2,PSI           SAVE IT
         LH 2,PSI            LOAD UPPER HALF OF PSI
         SH 2,ETA            SUBTRACT UPPER HALF OF ETA
         BNP SKIP1           IF NOT POSITIVE THEN SKIP OVER DIVIDE STEP
         LD 0,=D'1.0'        LOAD 1.0
         DDR 0,2             1.0/PSI IN FREG 0
         B SKIP2             SKIP AROUND THE LOAD RSAVE
SKIP1    LD 0,RSAVE          LOAD LAST VALUE OF R
SKIP2    MDR 2,0             MULTIPLY R*PSI
         LDR 4,2             LOAD R*PSI INTO FREG 4
         MDR 4,2             (R*PSI)**2
         MDR 4,2             (R*PSI)**3
         LDR 6,4             SAVE R*PSI**3 IN FREG 6
         MDR 4,2             (R*PSI)**4
         MD 4,=D'3.0'        3.*(PSI*R)**4
         AD 4,=D'1.0'        3.*(R*PSI)**4+1.0
         MD 6,=D'4.0'        4*(R*PSI)**3
         MD 6,PSI            4*(R*PSI)**3*PSI
         AD 6,ETA            4*(R*PSI)**3*PSI+ETA**2
         DDR 4,6             DIVIDE TO GET NEW R
*
         SDR 0,4             RSAVE-R
         LPDR 0,0            DABS(RSAVE-R)
         STD 0,TEMP1         SAVE TEMP1 (RSAVE-R)
         STD 4,TEMP2         SAVE TEMP2 (R)
         LH 8,TEMP2          LOAD UPPER PART OF TEMP2
         SH 8,TEMP1          SUBTRACT UPPER PART OF TEMP1
         CH 8,=X'0B00'       COMPARE WITH EXPONENT =11
         BH ROK              IF TEMP2-TEMP1>0B00 OK TO GO ON
         LDR 0,4             LOAD NEW GUESS FOR R INTO FREG 0
         LD 2,PSI            LOAD PSI INTO REG 2
         B SKIP2             LOOP AGAIN
*
ROK      STD 4,RSAVE         SAVE R
         STD 4,0(4)          RETURN R TO CALLING PROGRAM
         MD 4,ETA            R*ETA**2
         STD 4,0(5)          RETURN SIN**2
         SD 4,=D'1.0'        SUBTRACT 1.0
         LPDR 4,4            LOAD POSITIVE TO GET COS**2
         STD 4,0(6)          RETURN CSN
*
*RETURN TO CALLING PROGRAM
```

```
*
RETURN   L 13,SAV+4          LOAD ADDRESS OF SAVE AREA
         LM 14,12,12(13)     RESTORE REGS
         MVI 12(13),X'FF'    NORMAL RETURN
         BR 14 RETURN
*
*        IF ETA=0 THEN R=1/PSI,CSN=1,SN=0
*
ZERO     LD 0,=D'1.0'
         DD 0,0(2)           DIVIDE BY PSI
         STD 0,RSAVE         SAVE R
         STD 0,0(4)          RETURN R
         SDR 0,0             ZERO FREG 0
         STD 0,0(5)          RETURN SN=0
         LD 0,=D'1.0'        LOAD 1.0
         STD 0,0(6)          RETURN CSN=1.0
         B RETURN            RETURN TO CALLING PROG
*
*        STORAGE
*
         DS 0D
RSAVE    DC D'0.0'
PSI      DS D
ETA      DS D
TEMP1    DS D
TEMP2    DS D
         END
```

BIBLIOGRAPHY

Abramowitz,M. and Stegun,I.A. 1970. Handbook of Mathematical Functions, Dover Publications, N.Y.

Black,D.C. 1969. Nature 221,157.

Buccheri,R. 1976. The Structure and Content of the Galaxy and Galactic Gamma Rays, Goddard Space Flight Center, NASA Report CP-002, p. 52.

Cocke,W.J., Disney,M.J. and Taylor,D.J. 1969. Nature 221,525.

Daugherty,J.K. and Lerche,I. 1976. Phys. Rev D. 14,340.

Erber,T. 1966. Rev. Mod. Phys. 38,626.

Flowers,E.G., Lee,J-F, Ruderman,M.A., Sutherland,P.G., Hillebrandt,W. and Muller,E. 1977. Ap.J. 215,291.

Ginzburg,V.L. Zheleznyakov,V.V. and Zaitsev,V.V. 1968. Nature 220,355.

Gold,T. 1968. Nature 218,731.

Gold,T. 1969. Nature 221,25.

Goldreich,P. and Julian,W.H. 1969. Ap.J. 157,869.

Groth,E.J. 1975. Ap.J. Suppl. Ser. 29,431.

Hinata,S. 1973. Ap.J. 186,1027.

Hinata,S. and Jackson,E.A. 1973. Ap.J. 192,703.

Holloway,N.J. 1977. M.N.R.A.S. 171,619.

Holloway,N.J. 1977. M.N.R.A.S. 181,9p.

Jackson,A.E. 1976. Ap.J. 206,831.

Large,M.I. Vaughan,A.E. and Mills,B.Y. 1968. Nature 220,340.

Manchester,R.N. and Taylor,J.H. 1977. Pulsars, W.H. Freeman and Co., San Francisco, CA. p. 199.

Michel,F.C. 1975. Ap.J. 197,193.

Oegelman,H. Fitchel,C.E.,Kniffen,D.A.,Thompson,D.J. 1976. Ap.J. 209,584.

Pacini,F. 1968. Nature 221,454.

Radhakrishnan,V. and Cooke,D.J. 1969. Astrophys. Let. 3,225.

Roberts,D.H. and Sturrock,P.A. 1973a. Ap.J. 172,435.

Roberts,D.H. and Sturrock,P.A. 1972b. Ap.J.Let. 173,L33.

Roberts,D.H. and Sturrock,P.A. 1973. Ap.J. 181,161.

Ruderman,M.A. and Sutherland,P.G. 1975, Ap.J. 196,51.

Scharlemann,E.T., Arons,J. and Fawley,W. 1978. Ap.J. 222,297.

Shampine,L.F. and Gordon,M.K. 1975. Computer Solution of Ordinary Differential Equations: The Initial Value Problem, W.H. Freeman, San Francisco, Ca. 318p.

Smith,F.G. 1971. Nature Phys. SCi. 231,191.

Smith,F.G. 1973. Nature 243,207.

Smith,F.G. 1977. Pulsars, Cambridge University Press, Cambridge, Eng.

Staelin,D.H. and Reifenstein,E.C. 1968. Science 162,1481.

Sturrock,P.A. 1970. Nature 227,465.

Sturrock,P.A. 1971a. Ap.J. 164,529.

Sturrock,P.A. 1971b. Ap.J.Let. 169,L7.

Sturrock,P.A., Baker,K.B. and Turk,J.S. 1976,Ap.J. 206,273.

Tademaru,E. 1974. Ast. Sp. Sci. 30,179.

Thompson,D.J. Fichtel, C.E., Kniffen,D.A. and Ogelman,H.B. 1975. Ap.J.Let 200,L79.

Wallace,P.T. et al. 1977. Nature 266,692.